Glacier Image Velocimetry: an open-source toolbox for easy and rapid calculation of high-resolution glacier-velocity fields

Maximillian Van Wyk de Vries[1,2] and Andrew D. Wickert[1,2]

[1]Department of Earth & Environmental Sciences, University of Minnesota, Minneapolis, MN
[2]Saint Anthony Falls Laboratory, University of Minnesota, Minneapolis, MN

Correspondence: Maximillian Van Wyk de Vries (vanwy048@umn.edu)

Author's response

Contents of this pdf:

1. Response to Editor
2. Response to reviewer 1
3. Response to reviewer 2
4. Manuscript with tracked changes

We thank reviewers Ted Scambos and Anonymous reviewer 2, and editor Harry Zekollari for their insightful comments and suggestions. In addition to the changes described in the response to reviewers, the following edits to the manuscript have been made:

- Table 1 has been edited to include a brief description of the tools listed, as well as a flag for those that are freely available online.
- An additional table has been added to the supplementary materials to complement table 1, providing a link to the website or GitHub repository for each toolbox listed in Table 1. We hope that this will be a useful resource for new users looking to compare and contrast the capabilities of different toolboxes.
- Figure 1 has been expanded to include the name of the source code files used in each step. Along with the additional code changes and comments described in response to reviewer 2, we hope that this enables more computationally knowledgeable users to easily observe (and if desired, edit) the toolbox's structure.
- The colormaps in figures 7 and 10 have been updated to be legible to color-blind users, and in black and white copies
- The GIV GitHub repositiories and download links have been updated with the updated code. In particular, we have compiled a new Windows standalone app, and standalone apps for macOS and Linux (available at: https://doi.org/10.5281/zenodo.4147589).

Response to editor's comments

Editor comments are given in *italic*, author responses are in regular font.

A few comments from my side at this stage:

• I think that you argue well why 'The Cryosphere' is a suited journal: you do indeed present an easy-to-use GUI here, and the whole manuscript is very much centered around glaciology topics. In the end, you want to provide a tool that glaciologists can use to easily derive surface velocities, without having to look into the details/code behind this. It would, nevertheless, be good to have some additional graphical information about the structure of your code and the workflow in the main text to give the reader at least an intuitive feeling for what is going on 'behind the scenes'. The second reviewer suggests you to add such elements ('workflows' and 'dashboard'; Fig. 2 and Fig. 3 from Perks, 2020, GMDD are indeed good examples), but from your answer it was not entirely clear whether you plan to include this.

We thanks the editor for their positive comments, and for their thoughts on why 'The Cryosphere' is a suited journal. Our intention with Figure 1. of our manuscript was to serve a similar purpose to the flowcharts in Fig. 2 and Fig. 3 from Perks (2020). In order to improve the linkages between code an this workflow, we have added references to specific code functions within the figure. With these additions, we hope that users interested in following through the structure of the code may dig deeper (and further information is provided in the function descriptions and code comments). We also note that a full description of both the various functions and input parameter choices is provided within the user manual in supplementary material.

• You mention that "We were unable to locate a copy of PyCorr software on the internet (although it is mentioned in several papers, as you have highlighted), and are unsure if it is available for use by other teams": it would good if you could directly contact the people who developed PyCorr to clarify this, and (potentially) update your answer/manuscript based on this.

We have made several relevant updates to the manuscript, in particular indicating that while PyCorr is not abailable online, its derivative data products are (GoLIVE global glacier velocities). This has been highlighted in the edits to Table 1. We have included an additional supplementary data table, including a download link for each of the other toolboxes mentioned in Table 1 and some notes on relevant dependencies.

• From your answers it is clear that you will edit some figures in the updated manuscript. I hereby also appreciate that you took into account some of the initial editorial comments made during the 'access review'. It would also be good if the reviewers could answer some of the other (minor) issues that were initially raised (e.g. related to Table 1, rainbow colorbars,...etc)

The comments provided during the 'access review' have been taken into account while editing the manuscript and figures.

In particular we have changed the colormaps of relevant figures and added additional notes to Table 1 according to suggestions by both the editor and reviewers.

• *Removing the ice thickness reconstruction (as suggested by reviewer 1) is indeed fine, as it is more an application of what comes out of your toolbox than a result of the toolbox itself.*

We are glad that the editor agrees with these proposed changes, and have retained the portions of this section which we feel are useful for the testing and explanation of this toolbox (the velocity calculation of Chimborazo ice cap). The initial comments made by the editor on this section as well as comments by reviewer 1 have are being taken into account as we develop this work further.

Glacier Image Velocimetry: an open-source toolbox for easy and rapid calculation of high-resolution glacier-velocity fields

Maximillian Van Wyk de Vries[1,2] and Andrew D. Wickert[1,2]

[1]Department of Earth & Environmental Sciences, University of Minnesota, Minneapolis, MN
[2]Saint Anthony Falls Laboratory, University of Minnesota, Minneapolis, MN

Correspondence: Maximillian Van Wyk de Vries (vanwy048@umn.edu)

Final response - Review 1

Reviewer comments are given in *italic*, author responses are in regular font.

The study describes a new ice-velocity mapping toolkit using visible – near-infrared image pairs or multiple images spanning a range of time. The authors have applied several well-used and a few clever filtering and information-extraction methods in the toolkit. It is good to have one software package that provides both the vectors and a thorough means of editing them in one workflow. The authors then demonstrate the value of the velocity mapping with a group of case studies spanning the range of glacier and small ice cap environments in the northern hemisphere and a tropical location.

This is a well-written paper, and the method seems sound and very useful, although there are several similar tools available at this time. This should be published with minor revisions. The only major change I suggest is removing the ice thickness estimation and place it in another paper with other similar targets so that the calculations will be more visible to the community. It is not necessary to place it in this method-and validation paper. I make several significant suggestions for the abstract as well, and many further suggestions in the rest of the text.

We thank Dr. Ted Scambos for the positive comments about the method and manuscript, as well as the useful suggestions. We have made several key changes to the manuscript based on the recommendations in this review, in particular:

1. We added a number of key references.
2. We rewrote of the abstract based on your suggestions.
3. We removed the section on ice thickness inversion, which will be developed into its own manuscript (see detailed comments below)
4. We edited our figures for clarity.

In general, references should be listed in time order, from earliest publication date to most recent. Adopting this convention will mean several minor changes in the manuscript.

We have verified that all references are now listed in chronological order.

Suggested changes to Abstract: We present 'Glacier Image Velocimetry' (GIV), an open-source and easy-to-use software toolkit for rapidly calculating high spatial resolution glacier-velocity fields. Glacier ice velocity fields reveal their flow dynamics, ice flux stability, and (with additional data and modelling) ice thickness. Obtaining glacier velocity measurements over wide areas with field techniques is labour intensive, and often a safety risk. Recent increased availability of high-resolution, short-repeat-time optical imagery allow us to obtain ice displacement fields using 'feature tracking' based on the presence of persistent irregularities on the ice surface, and hence, velocity over time. GIV is fully parallelized, and automatically detects, filters, and extracts velocities from large datasets of images. Through this coupled toolchain and an easy-to-use GUI, GIV can rapidly analyze hundreds to thousands of image pairs, requiring only a moderately high-end laptop or desktop computer. We present four examples of how the GIV toolkit may be used: to complement a glaciology field campaign (Glaciar Perito Moreno, Argentina), calculate the velocity fields of small (Glacier d'Argentière, France) and very large (Vavilov ice cap, Russia) glaciers, and determine the ice volume present within a tropical ice cap (Volcán Chimborazo, Ecuador). Fully commented code and a standalone app for GIV are available from GitHub and Zenodo.

We are very grateful for this re-write of our abstract, and adopt it with a few minor changes (in particular to reflect the removal of the ice thickness/volume calculations).

Consider adding these very pertinent additional references in the introduction Line 20-21 : Howat, I.M., Porter, C., Smith, B.E., Noh, M.J. and Morin, P., 2019. The Reference Elevation Model of Antarctica. Cryosphere, 13(2), https://doi.org/10.5194/tc-13-665-2019 Scambos, T.A., Haran, T.M., Fahnestock, M.A., Painter, T.H. and Bohlander, J., 2007. MODIS-based Mosaic of Antarctica (MOA) data sets: Continent wide surface morphology and snow grain size. Remt. Sens. Env., 111(2-3),242-257, https://doi.org/10.1016/j.rse.2006.12.020. Line 32: Stearns, L.A., Smith, B.E. and Hamilton, G.S., 2008. Increased flow speed on a large East Antarctic outlet glacier caused by subglacial floods. Nature Geoscience, 1(12), 827-831, ://doi.org/10.1038-/ngeo356. Line 42: Bindschadler, R.A. and Scambos, T.A., 1991. Satellite-image-derived velocity field of an Antarctic ice stream. Science, 252(5003), 242-246, https://doi.org/10.1126/science.252.5003.242. Line 47: Fahnestock, M., Scambos, T., Moon, T., Gardner, A., Haran, T. and Klinger, M., 2016. Rapid large-area mapping of ice flow using Landsat 8. Remt. Sens. Env., 185, 84-94, https://doi.org/10.1016/j.rse.2015.11.023.

We agree that these references provide important background information, and have added them to our introduction.

Line 52: you may want to note these two data sites, presenting already-processed data – https://nsidc.org/data/golive https://nsidc.org/apps/itslive/

We have added a one sentence description of these datasets, as they are likely of interest to the readers of this paper (and may be a viable substitute for running GIV over large regions, and where lower spatial and temporal resolution are acceptable).

Table 1: PyCorr is the tool behind Fahnestock et al., 2016, which produced some of the mosaics in Gardner et al., 2018.

We have add PyCorr to the table, along with 3 other tools that were flagged by reviewer 2 (Pointcatcher, PyTrx and EMT). We have also added a sentence to the table description to highlight that our list is not exhaustive. We were unable to locate a copy of PyCorr software on the internet (although it is mentioned in several papers, as you have highlighted), and are unsure if it is available for use by other teams.

Line 117 – you say 'multipass methods take advantage of the reduction in chip size to improve the signal to noise'. I think this needs to be rephrased – in general, if there is low shear or deformation across the scene, large chip sizes produce much better matches.

We have expanded and clarified the benefits of multipass methods in the following sentences: "Multi-pass methods refine displacement estimates in multiple iterations, refining initial coarse window size displacement calculations with progressively smaller window sizes. Multi-pass methods combine the advantages of better feature matching at large window sizes with the higher spatial resolution of small window sizes. Both methods are integrated into GIV, which uses a 3 iteration multi-pass algorithm."

We have also added a reference in the methods section to a recent PhD thesis by Dr. Bas Altena (2018), which provides a well written and detailed background on some of the common processing steps in glacier feature tracking.

Line 150 – at what 'scale' or number of grid cells are these statistical values calculated? I would assume this scale is either set by the user or by some extracted geography of the ice within the image pair(s).

The statistical values are calculated for a single cell, averaged through time. For clarity, the sentence was changed to : "Secondly, GIV calculates the mean, standard deviation, median, minimum, and maximum velocities through time at each grid cell in the dataset."

Figure 5 – label the color bars, with 'Flow Speed' and 'Bearing... Could also add degree symbols to the bearing indices,

The recommended changes have been made.

Figure 7 – the perspective view is a bit difficult to follow without somewhat more area covered to gain a feel for the 3-dimensional structure... The figure is nice but takes a while to orient mentally. Expand view, or, a second inset that shows the

map view?

This figure has been edited to include a second inset showing the full-glacier velocities in map view. The color scheme has also been changed (from https://colorbrewer2.org/) in order to be 1) suitable for converting to black and white and 2) color-blind friendly, as recommended by the editor.

Figure 8 – Expand the velocity scale (taller) in one of the top two insets, and no need to repeat it in both (a) and (b). The titles of (a) and (b) should be 'ice speed' unless you include a few vectors for direction. Include the month of the velocity mapping in the 'title' of the insets for (a) and (b).

The velocity scale has been expanded, labelled as 'Flow speed (m/yr)', and is no longer duplicated. The velocity maps are full yearly averages (well, March-September due to the Arctic winter), and so do not correspond to a specific month. They have been labelled as yearly averages.

Line 263 – suggest change to '....or ice basal conditions are identified.'

The recommended change has been made.

Figure 9 – What is the difference, exactly? GIV minus Zheng or Zheng minus GIV?. The scale of the speed differences is large for the margins, and appears to be locally consistent. However it does not extend outside of the glacier boundaries, so it would seem that its not due to a rotational mis-registration. It would seem that somehow the two mappings captured a true physical shift in the margins or speed profile across Vavilov during May 2017 somehow.

We have edited the figure caption to clarify the difference map, it now reads: "a) shows a difference map, corresponding to Zheng et al. velocity minus GIV velocity"

We have also been in touch with the creator of the Vavilov velocity maps (Whyjay Zheng) and it indeed seems likely that the difference may be resolving a real shift in margin position and/or velocity over time. It is relevant to note that a project comparing results from GIV and other feature tracking tools (including Zheng et al's CARST) to glacier GPS data is ongoing.

Lines 268-269 – Was geolocation necessary? Landat 8 geolocation is generally within 5 meters, i.e. significantly less than a panchromatic band pixel; Sentinel-2 image geolocation is similar. What was the scale of the error in geolocation that you corrected?

Geolocation shift was small, on the order of half a velocity pixel to one velocity pixel ($\sim$50-100m). GIV velocities were derived from non-georeferenced imagery (.jpg) and georeferenced based on corner coordinates, which likely contributed to the

mis-match. An option to run GIV directly on geotiff images has since been added.

Line 272 – remove 'total', makes it sound like you are summing the velocities... note also, it's speed, not velocity: velocity is a vector.

The recommended change has been made, and 'velocity' changed to 'speed' where referring to the magnitude only.

Line 290 – please provide the lat long for Chimborazo, and for the other sites (sorry if I missed it).

The coordinates of all locations have been added.

Line 295 – change to '...but for this single point (which we use for benchmarking our method), combined with..."

Lines 306 – 316: Hmm. Do you not have a thermal profile from the 54 meter core to the base? It is very likely that the base of the ice is warmer than the air-temperature-based isotherm because of insulation. Moreover, the presence of water-logged ice (a firn aquifer) means that it is likely that water drains to the bed – and further, you note that the glacier supplies water to the local watershed so seasonal melting is significant (and in general, meltwater on a glacier finds its way through the ice and to the ice-bedrock interface, warming the bedrock.

We agree with these comments, and will bear them in mind when further developing the ice thickness inversion work. In the meanwhile, the associated lines have been removed from the manuscript.

Rather than take on this complex mountain glacier, why not apply your method to the Vavilov Ice Cap outside of the area of sudden rapid flow? Or you might try a glacier where it is more certain that <0C conditions exist at the bed, and with more validation data – Commonwealth Glacier or Canada Glacier in the Dry Valleys would be good.

More generally — this paper does not need this section on thickness estimation – your point is to show off the quality and extent and usefulness of the GIV data, and the extensive processing and filtering steps you take – and while this is a demonstration of 'usefulness', it's better as a stand-alone study of Chamborazo or a small set of glaciers where the result will not be lost in the literature (no one will find your thickness estimate in this paper). A series of ice thickness estimates for cold-based Andean glaciers, or Dry Valley glaciers, or selected Himalayan glaciers, using GIV, would be cited extensively.

Since the submission of this manuscript we have run variations of this methodology on 6 additional tropical ice caps in Ecuador and Colombia, including some glaciers with better ground-penetrating radar derived ice thickness constraints. Following your suggestions, we crop out the discussion about inverting for ice thickness, and will place this in a separate paper with more

space for discussing the inversion parameters and model-data comparison. We have kept the Chimborazo ice velocity results in this paper, as we feel it is a useful example of using GIV at small and slow-moving glaciers.

Line 322 – re-write, confusing. Maybe you mean: local -basal- stresses induced by the ice are much greater than lateral stresses between columns of ice...?

Line 340 – 3090 Sentinel -2 image pairs in 2 hours on a Dell laptop – did you subset the Sentinel-2 to just cover the Chimborazo summit area? I am also surprised there are that many pairs – you might include a statement as to how many distinct images were processed.

This sentence has been edited for clarity. There are 91 unique images, which are cropped to the region surrounding Chimborazo (with enough bare rock to enable the stable ground correction) and paired up into all possible pairs with >6 months separation. In theory there are $(n^2-n)/2$ possible image pairs, or 4095 total image pairs in this case (and around 1000 images pairs are excluded due to a separation of <6 months).

Lines 344-355 – There is no need for all this speculation on your ice thickness estimate in this paper – this belongs in a separate paper where the approach can be developed more and applied to a set of related areas (perhaps). I strongly suggest cutting this ice thickness section out and placing it in a separate paper. I think it might be interesting to apply GIV to an ice sheet region such as Nimrod Glacier or Peterman Glacier.

As mentioned above, we have limited the Chimborazo section to the calculation of ice velocities and will develop the thickness inversion methodology into a stand-alone paper. We have tested GIV on Antarctic Peninsula glaciers and portions of Thwaites glacier calving front (with no issues). Nimrod glacier appears to be an interesting case study due to its large central nunatak, and good baseline data from Stearns (2007, PhD thesis; 2011).

Line 390 – change to '...alternative. GIV is easily learned and is not computationally time-consuming, and the results...' Not to be harsh, but GIV itself does not learn, and doesn't run either.

We have corrected our sentence.

Glacier Image Velocimetry: an open-source toolbox for easy and rapid calculation of high-resolution glacier-velocity fields

Maximillian Van Wyk de Vries[1,2] and Andrew D. Wickert[1,2]

[1]Department of Earth & Environmental Sciences, University of Minnesota, Minneapolis, MN
[2]Saint Anthony Falls Laboratory, University of Minnesota, Minneapolis, MN

Correspondence: Maximillian Van Wyk de Vries (vanwy048@umn.edu)

Final response - Review 2

Reviewer comments are given in *italic*, author responses are in regular font.

The toolbox presented by the authors is a GUI to ease feature tracking routines within a MATLAB environment. The naming of the toolbox is a reference to Particle Image Velocimetry (PIV), which is a well established technique within fluid mechanics. It is based upon particle seeding within a fluid, illuminated by light behind a narrow slit to get a within-plane velocity profile, thus in a well-controlled environment. When particles are not well stirred, have a lot of out-of-plane displacements, too large time separation, or other effects complicating the tracking: the experiment is done all over. The authors lend the methodologies from this domain, and implement this on natural environment to extract glacier surface velocity. This transfer is more complicated as it might initially seem to be, as seeding is absent (though people in hydrology are experimenting on this issue [Pizarro et al. 2020]), and more importantly experiments can't be redone.

The toolbox has some application specific adjustments, which is in line with other application domains, where similar toolbox are introduced, such as: Optical tracking velocimetry (OTV) [Tauro et al 2018], Surface Structure Image Velocimetry (SSIV) [Leitaoa et al. 2018], Kanade–Lucas Tomasi Image Velocimetry (KLT-IV) [Perks 2020], Part2Track [Janke et al. 2020], TecPIV [Boutelier 2016], Rectification of Image Velocity Results (RIVeR) [Patalano et al. 2017], Waves Acquisition Stereo System (WASS) [Bergamasco et al. 2017], or more specific to glaciers: Environmental Motion Tracking (EMT) [Schwalbe et al. 2017], PyTrx [How et al. 2020], Image GeoRectification and feature tracking toolbox (IMGRAFT) [Messerli et al. 2015], Pointcatcher [James et al. 2016]. Given the list above, and the journals where these toolboxes are presented, it might be a valid question why the authors have opted for a submission to The Crysophere, and not a technical EGU journal like Geoscientific Instruments or Geoscientific Model Development?

We thank the reviewer for their detailed review. We would specifically like to thank the reviewer for taking the time to read through GIV's code, as their recommendations have helped improve both the manuscript and the toolbox itself. We have taken the time to review each comment and recommendation in detail, and have made some moderate to substantial changes to GIV's code. We hope that this response clarifies some of our choices, and highlights the changes made.

The main modification which have been made to the code are:

1. We review the entire code to improve the code formatting (removal of unnecessary spaces and tabs) and increase the number of comments. We do not expect a large proportion of GIV's users to be reading through the entire code, but aim to make it accessible for when they do (and make it possible for users to use our functions in their own tools).

2. We change the format of our inputs array (which stores the input parameters) from a MATLAB cell array to a MATLAB struct array. The struct array uses dot notation to make it more human-readable, and should make the code more accessible (e.g. changed from 'inputs{30,2}' to 'inputs.parralelize').

3. We implement an option to read in images directly as geotiff images and preserve the geographic information throughout processing. If users input geo-tiffs they do not need to input corner coordinates.

4. We review the calculation of circular statistics (flow direction mean and standard deviation), and edit Dr. Berens' CircStat toolbox to tolerate NaN values.

5. We re-compile the Windows standalone app with the changes, and compile additional apps for macOS and Linux.

We describe the changes in more detail below, and respond to specific review comments. We have added reference to the relevant toolboxes you have listed in this paragraph as well.

To briefly touch on the decision to publish in The Cryosphere (TC) rather than a technical journal, the primary objective of our toolbox is to be accessible to glaciologists who may not otherwise be involved in feature tracking. We hope that GIV will bridge a gap between coarser resolution global glacier surface velocity datasets (e.g. GoLIVE, ITS_LIVE) and the more localised, higher resolution data required by some studies or field campaigns. Other good feature-tracking toolboxes do exist (see table 1 for many of them), but can be challenging to use with no computational or remote sensing background. GIV is easy to install, quick to learn, and quick to run, without requiring background knowledge of how the code runs (including by students). We believe that the manuscript is well within the scope of TC, and that publishing in TC will better reach the intended audience of this paper than technical journals. In addition, we believe that the case studies presented here will be of interest to the glaciological readership of TC.

We should note that we did share your concerns at the outset, and indeed contacted the editorial staff at The Cryosphere about appropriate fit before submission. Their support for our submission was also key to this being the chosen venue for the paper. This is often a difficult choice when presenting a paper focused on both the application and its methods, and we appreciate the acknowledgment of this.

There are some implementations which one could expect for a toolbox tailored towards glaciology to be presented, but are not included. In addition some features are included, which need further assessment, to highlight their improvement, if they do.

We thank the reviewer for highlighting some recommended changes. We describe the changes we make to the code in this

response.

To be more specific the comments are grouped into different paragraphs: Analysis of the 10-bit data of Landsat 8 [Jeong et al. 2015] and Sentinel-2 [Kääb et al. 2016] over dark overshadowed terrain have shown there is a significant benefit over 8bit data. Why do the authors downgrade their imagery to 8-bit RGB? In the same line, the use of non-georeferenced ".jpg" or ".png" data is strange. MATLAB supports mapping tools for such issues, why are these not adopted. While the toolbox needs a specific dimension in order to work, it is very strange this is not present in the toolbox. The choice of using angles (lat,lon) for metric data is confusing.

In brief, the changes we make to the code now make it possible to run georeferenced, 10 bit geotiff datasets. When applying an orientation filter to the data (e.g. the NAOF we have implemented), we find little difference between 8 bit and 10 bit data even in shadowed/clouded areas. The orientation filter tends to cancel out contrasts within the data. The 10 bit data may prove advantageous where orientation filtering is not suitable and simple low-pass filtering and/or contrast limited histogram equalization (CLAHE) is used.

The authors present a new image transform dubbed "NAOF", but is there a significant improvement, over for example typical orientation filtering approach? At least to me, the 45 degrees filters seem like a redundant feature, as 90deg angled steerable filters incorporate all information [Freeman et al. 1991]. It seems the implementation is a combination of work similar to [Ahn et al. 2011], and orientation filtering [Heid et al. 2012]. But it is questionable, if the additional calculations add towards improvement. The filter banks are correlated (as just mentioned), furthermore, the visible bands are similiarly correlated over glaciers. Hence, the information gain might be very limited.

We tested a number of different kernels for the orientation filter, and found that some of the simpler orientation filters would enhance and suppress features (particularly crevasse fields) depending on their orientation. The filter banks are correlated, but adding both the 90 degree and 45 degree filters preserves more feature uniqueness than either alone. This is important for reducing the number of false matches and signal to noise ration in crevasse fields, where subsequent crevasses have similar orientation signals. The visible bands are correlated, which is why we sum them into a single band. On some glaciers we have found that near infrared Band 8 of Sentinel 2 (842 nm) may produce a better feature contrast than other bands on some glaciers. We have also found that shortwave infrared bands 10 and 11 (1375 and 1610 nm) can be suitable in some cases (high contrast between ice and supraglacial debris), however suffer from a lower spatial resolution. Different band combinations can easily be created within SentinelHub (which we discuss briefly in the user manual). We mostly use contrast-enhancing SentinelHub custom script (javascript) which combines Sentinel 2 bands 3,4 and 8. We will add this custom script to a GitHub repository.

The paragraph on velocity calculations talks about two methods to extract displacements from an image pair. However, this distinction is more about the option if refinement is applied or not. The authors limit themselves to frequency domain methods,

which is the de-facto procedure for PIV. However, spatial domain methods can be more favorable for glacier related applications. This comes down to the point given above, of the transfer from fluid mechanics towards an application domain without the ability to redo an experiment. Hence, the velocity profile can be highly variable (extensive shear, valley walls, diverging flow, fast flow, ...). Spatial domain methods are more resistant to shear flow, the chip is not related to the search space (as with fourier methods). The authors might have considered spatial domain methods, but for clarity it might be fruitfull to mention this, and why. In PIV experiments, one is able to adjust the image sampling rate, to be in accordance with the maximum flow velocity, this is less the case for glaciers.

At the early stages of this toolbox we investigated both frequency domain and spatial domain (Normalized Cross Correlation) matching algorithms. In particular we tested the NCC option within IMGRAFT (Messerli and Grinsted, 2015) and 'discrete cross correlation window deformation' option in PivLab (Thielicke and Stamhuis, 2014) which allows for shearing of features. We found no clear improvement in matches relative to frequency domain cross correlation even in areas with significant ice shear (glacier margins with around 1000 m/yr velocity gradient across one kilometre). We also found that the multi-pass frequency domain matching would usually outperform single passes in both frequency and spatial domain. However, we found that changes to the pre and post-processing would often have the greatest improvement on final velocity maps, so have emphasized this aspect in GIV. This is indeed less of an issue within fluid dynamics where the sampling rate, tracers and illumination may be controlled.

We have added two sentences explaining why we opt for frequency domain methods in GIV, and some of the relative benefits of each method. We also refer readers interested in further discussion to Thielicke and Stamhuis (2014) and a chapter of a recent PhD thesis by Altena (2018) which provides an accessible and detailed discussion of these topics from the perspective of glaciology.

Technical comments: In general the code is very messy, many duplicate lines exist, commenting is absent ("strcmpi(inputs{51,2}, 'Yes')"). At multiple locations indents are used in-appropriately. Documentation and commenting within the code is limited. Every function has an extensive help section, which is typically an acknowledgment and info about GIV. Input or output variables are not described. For many or all functions, tests are lacking. Factorization is on a low level. Given this situation of the code, how do the authors see adoption by others? The objective of the authors is to be a wrapper (based upon ImGraft and matPIV), then one would expect documentation to be extensive.

We would again like to thank the reviewer their time taken providing feedback on our code. We have inspected every function in GIV to improve formatting (tab only within loops, no unnecessary spaces, etc.), increase the number of in-code comments, and add to function descriptions. As mentioned above, reading the code is not necessary for running GIV (and is not possible in the case of the standalone apps). As such we do not believe code commenting is an important factor for the adoption of GIV by others. However, we aim for our code to be scrutable by those that do wish to read it, or wish to use our filters within their own code.

A number of the 'duplicate lines' within the code are present in order to enable the various input options. We hope that the additional comments throughout the code, alongside the change of our inputs array to a dot notation struct array will make these clearer. For example "strcmpi(inputs{30,2}, 'Yes')" should now read "strcmpi(inputs.parralelize, 'Yes')" and be accompanied with at least a brief comment.

Sub-pixel: There does not seem to be a sub-pixel estimation present? Why is this?

A sub-pixel estimation is present. For the single-pass algorithm it is built into the 'GIVtrack.m' function, while for the multi-pass algorithm a separate function ('GIVtrackmultipeak.m') is called within the final feature tracking pass ('GIVtrackmulti-final.m'). The multi-pass (recommended) sub-peak finder is set to a gaussian peak fit by default (and in the app), but can be modified to a centroid or parabolic fit within the code if desired. We have found that changing this has little effect on outputs.

The domain of PIV is also extensively populated with papers about peak-locking, it would be good if the authors put some effort in this as well. This bias is especially present in sub-pixel estimation directly done on the correlation surface. Other methods, such as TPSS, as implemented in Cosi-Corr are less sensitive to this effect (which to a large extent might explain its popularity in geodetic imaging).

We have not investigated peak-locking in detail while working on GIV. Inspection of raw displacement and velocity histograms shows only a minor bias towards integer values, and does not appear to be a major source of error.

A project is currently underway comparing feature tracking results from GIV and other feature tracking toolboxes to GPS derived velocity data. We are planning on considering the effect of different sub-pixel estimation schemes, and future versions of GIV will be updated if a particular algorithm is clearly superior. An in depth discussion of the particle tracking parameter options is beyond the scope of this manuscript.

Geo-referencing: The gridspacing as it is implemented now assumes all rectangular and upright pixels, please adjust this.

As mentioned above, we have added an option for GIV to process raw geotiff data and read in geographic data off the images.

If this comment is referring to the velocity fields being projected onto a horizontal plane (i.e. not corrected for topographic strike and dip), this is common practice in feature tracking. This correction may be applied using a DEM after running GIV, but is usually very small.

Matlab: To my knowledge Matlab is not open access, the code might be open, but many of the algorithms are hidden away and licensing is needed. Hence, I am not so sure if the description about FFTW is needed, as one is not able to access this. Secondly, it is a standard routine within MATLAB.

FFTW is an open source toolbox, however this is correct about much of MATLAB. The objective of this paragraph is to provide some justification for the toolbox being coded in high-level interpreted programming language MATLAB. FFTs constitute the largest computational expense of feature-tracking models, and in MATLAB are performed efficiently in C subroutine library FFTW rather than in any native MATLAB code. As such, GIV can process feature tracking pairs rapidly (particularly with the built-in parallelisation).

Merging satellite data: The authors describe a time-series construction method, illustrate a toy example. But it seems they apply a sigma-filter, and do simple infilling. There are more advanced methods available, which are more adaptive towards velocity data. Hence, a simple reference to (e.g.: [Mouginot et al. 2017]) might suffice for the implementation here, and this section can thus be reduced considerably.

The temporal sampling is a bit counter intuitive, as this is an opposite direction to the workflow of [Millan et al. 2019]. Where they found the time-span needs to be of sufficient size, in order to be of most use. Why then do the authors prefer the shorter time steps?

We do not fully understand the above comments. Our findings on optimal temporal sampling are in line with Millan et al., 2019, and we by default exclude velocity image pairs with temporal separation of less than one week. We describe the example of a very slow moving glacier in the Chimborazo case study, where excluding time steps shorter than 6 months provided the best velocity results. The minimum and maximum time separation limits can be adjusted within the user interface according to the specific characteristics of the glacier of interest.

If this comment is referring to the first iteration of monthly timeseries generation, the 0-1 scoring system refers to the proportion of a velocity map within a given month rather than the temporal separation. A 7 day or 30 day separation velocity map entirely within a given month will both be assigned a score of 1. Velocity maps overlapping into other months will be assigned lower scores.

The sigma-filter and infilling are post-processing steps to improve the quality of individual monthly maps.

Other averaging and timeseries generation methods for glacier velocities are available (e.g. Millan et al., 2019's NetCDF Geo-Cubes, Altena et al., 2019's Hough space method, etc.), although do not inherently generate monthly time-series. Our method generates a full dataset mean and median, as well as monthly velocity maps which (we hope) are easier to interpret than the unevenly sampled satellite image pair timing.

Code specific: There is a function about intensity capping, while this might be of interest to PIV, it is questionable if this is of interest to environmental signals. Bright intensity of seed points within dark water are very much different from glacier surfaces. Also how does this merge with the high-pass filtering... ?

Intensity capping is not usually necessary, but can be useful where bright snowpatches are present close to a debris covered or otherwise dark glacier. In general the filters do not need to all be applied or stacked. By default only the orientation filter is applied. My recommended filter choices are:

- Orientation filter (NAOF) only = default
- High-pass filter and CLAHE (+ Sobel filter in some cases) = where orientation filtering creates too much noise
- Intensity cap + High-pass filter and CLAHE (+ Sobel filter in some cases) = where bright patches are present, and orientation filtering creates too much noise

Users may wish to experiment with a small dataset, different glaciers will have different optimal pre-processing parameters.

Even though your algorithms are optimized, they might not pull out the best of the machinery, yet. For example, the function "neighbourfilter" contains a double loop, to process a kernel. An internal function of Matlab called "nlfilter" might be much faster. A good reference for such implementations can be found in "Accelerating MATLAB Performance" (http://undocumentedmatlab.com/books/matlab-performance). In the same function from line 95 onward, the authors use double indexing. While linear indexing is possible as well, which make vectorization possible (which is MATLABs strong point). This greatly improves the processing time as well.

We thank the reviewer for the useful reference and recommendations. We test an implementation of 'neighbourfilter.m' using nlfilter, however it results in little overall speed-up and some unexpected artefacts. The artefacts can probably be fixed by re-writing the function around nlfilter, however due to the small overall increase in efficiency we leave the function as is for now. We believe that the inclusion of parallel computing of feature-tracking pairs is likely to result in the greatest computational speed-up relative to other tools.

I am not sure if the variance calculation of the flow direction is calculated correctly. Offsetting the direction and applying a weighting might work, but maybe correct circular statistics might be more appropriate, see [Berens 2009] for a toolbox implementation. It might be more easy to use the mapping coordinates instead...?

Our flow direction mean calculation appears give the same results as Berens's CircStat on examples tested, but are not sure of its behaviour in all scenarios. Thus, we replace it with the well-tested CircStat.

We make several changes to CircStat to enable calculation of mean and standard deviation in data containing Not a Number (NaN) values. We will share the NaN tolerating version of the toolbox on GitHub or file exchange.

It might be good to give an example; here is a sniplet of your code (a straight copy):
if smoothsize == 2;

mask = [0 1 0; 1 0 1; 0 1 0];

elseif smoothsize == 3;

mask = [0 1 0;1 1 1; 1 0 1; 1 1 1; 0 1 0];

elseif smoothsize == 4;

mask = [0 0 1 0 0 ;0 1 1 1 0 ;0 1 1 1 0; 1 1 1 1 1 ; 0 1 1 1 0; 0 1 1 1 0; 0 0 1 0 0];

elseif smoothsize == 5;

mask = [0 0 1 0 0 ;0 1 1 1 0 ;0 1 1 1 0;1 1 1 1 1 ;1 1 1 1 1 ; 1 1 1 1 1 ; 0 1 1 1 0; 0 1 1 1 0; 0 0 1 0 0];

end

why isn't this in a function? Something like: function [mask] = make_mask(smoothsize)

"

generates a neighborhood kernel in the form of a diamond,

though excludes the central pixel

input:

smoothsize - integer value

output:

mask - logical array

"

if nargin<1, smoothsize = 3; end

mask_radius = floor(smoothsize/2);

mask = strel('diamond', mask_radius); % make a diamond shape

mask = mask.Neighborhood;

mask(mask_radius+1, mask_radius+1) = 0; % exclude the central element

end

That function is indeed much more elegant and flexible than our implementation. We have implemented it in the code (with due acknowledgement) and hopefully it makes the filter more flexible for other uses.

In all I am aware this is, like all research, work in progress, and I think this is a very useful direction. But in its current state and form, sufficient work needs to be done to be of interest, please see [Perks 2020] for a nice example. Here workflows are nicely presented, a dashboard is present, etc. All in all, I think a transfer towards a technical journal of EGU might be more in place.

We hope that the comments and code edits presented clarify our decision to submit to The Cryosphere, and answer some of the concerns presented in this review.

Textual: p63: "broken down" is misleading, as overlapping chips can also be used p140: superscript the 2, to make it a square

The recommended changes have been made.

Glacier Image Velocimetry: an open-source toolbox for easy and rapid calculation of high-resolution glacier-velocity fields

Maximillian Van Wyk de Vries[1,2] and Andrew D. Wickert[1,2]

[1]Department of Earth & Environmental Sciences, University of Minnesota, Minneapolis, MN
[2]Saint Anthony Falls Laboratory, University of Minnesota, Minneapolis, MN

Correspondence: Maximillian Van Wyk de Vries (vanwy048@umn.edu)

Abstract. We present 'Glacier Image Velocimetry' (GIV), an open-source and easy-to-use software toolkit for rapidly calculating high spatial resolution glacier-velocity fields. Glacier ice velocity fields reveal ~~their~~ flow dynamics, ~~ice flux stability~~ice-flux changes, and (with additional data and modelling) ice thickness. Obtaining ~~glacier velocity~~ glacier-velocity measurements over wide areas with field techniques is labour intensive ~~,~~and often a safety risk. Recent increased availability of high-resolution, short-repeat-time optical imagery allow us to obtain ice displacement fields using 'feature tracking' based on the presence of persistent irregularities on the ice surface, and hence, velocity over time. GIV is fully parallelized, and automatically detects, filters, and extracts velocities from large datasets of images. Through this coupled toolchain and an easy-to-use GUI, GIV can rapidly analyze hundreds to thousands of image pairs on a laptop or desktop computer. We present four ~~examples of how~~ example applications of the GIV toolkit ~~may be used: to~~ in which we complement a glaciology field campaign (Glaciar Perito Moreno, Argentina) ~~,~~ and calculate the velocity fields of small (Glacier d'Argentière, France) and very large (Vavilov ice cap, Russia) glaciers ~~, and~~ as well as a tropical ice cap (Volcán Chimborazo, Ecuador). Fully commented code and a standalone app for GIV are available from GitHub and Zenodo.

1 Introduction

Satellite imagery revolutionized our ability to study changes ~~in~~ on the surface of our planet. Satellite datasets now routinely support storm and drought evaluations (Klemas, 2009; Rhee et al., 2010; AghaKouchak et al., 2015), volcanic activity monitoring (Wright et al., 2002; Harris, 2013), and landslide-hazard analysis (Metternicht et al., 2005; Tralli et al., 2005; Marc and Hovius, 2015). In glaciology, remote sensing has enabled global glacier inventories (Pfeffer et al., 2014; Earl and Gardner, 2016) as well as high-resolution elevation models and image mosaics of the Antarctic and Greenland ice sheets (Bindschadler et al., 2008; Hui et al., 2013; Howat et al., 2014; Porter et al., 2018). With temperatures consistently rising throughout much of the globe, these images also provide an important temporal record of changes in ice extent and volume, as well as an effective tool for communicating these changes to the broader public (Scambos et al., 2007; Stocker et al., 2013; Howat et al., 2019).

The use of imagery is not limited to mapping changes in glacial extent. The snowline on temperate glaciers, easily visible from end-of-melt-season images, defines the equilibrium-line altitude, thereby delineating glacier accumulation and ablation areas (Bamber and Rivera, 2007; Rabatel et al., 2008; Yuwei et al., 2014). Identifying both seasonal and annual changes in snowline can provide important information about local winter precipitation, summer air temperatures, and longer-term glacier mass changes (Bakke and Nesje, 2011).

Velocity measurements permit scientists to map glacier divides and drainage basins (Davies and Glasser, 2012; Pfeffer et al., 2014; Mouginot and Rignot, 2015) and track changes in surface melt production and accumulation (Mote, 2007; Sneed and Hamilton, 2007). Advancing techniques to remotely sense glaciers – and particularly their velocities – continues to provide new avenues to address key questions in ice dynamics and the future of glaciers under a changing climate (Stearns et al., 2008; Wal et al., 2008; Rignot et al., 2011; Willis et al., 2018). Even the earliest glaciologists identified that glaciers may flow as viscous fluids (Forbes, 1840, 1846; Bottomley, 1879; Nye, 1952), and later that ~~glacier surface motions are~~ glacier-surface motions reflect a complex interplay between internal deformation, basal sliding, and deformation of subglacial sediments (Deeley and Parr, 1914; Weertman, 1957; Kamb and LaChapelle, 1964; Nye, 1970; Fowler, 2010). Sudden peaks in velocity may result from a sudden change in basal sliding, perhaps as the result of changing englacial hydrology. Long-term speedups or slowdowns may reflect climatic shifts or drainage reorganizations.

Deriving glacier velocities from satellite imagery is possible through an image-analysis technique known as 'feature tracking', 'image cross correlation', or 'particle image velocimetry'. The latter term, 'particle image velocimetry', describes a well-established technique in fluid dynamics, typically involving the use of a high-speed digital camera to track the motion of tracers within a fluid in a laboratory setting (Buchhave, 1992; Grant, 1997; Raffel et al., 2018) . These ideas were first carried over to the field of glaciology by Bindschadler and Scambos (1991) and Scambos et al. (1992) to evaluate the flow velocity of a portion of an Antarctic ice stream. Since that time, the increasing abundance and availability of imagery has facilitated expanded use of ~~feature tracking-based~~ feature-tracking-based velocimetry techniques. With the release of the full Landsat data archive and launch of Sentinel-2, ~~10-30 m~~ 10–30-m pixel resolution imagery of any given location is now available at sub-weekly repeat coverage intervals. A number of studies ~~use this exceptional potential to map the velocity of~~ apply this exceptional archive to map velocity fields across the major ice sheets as well ~~as~~ those of many glaciers around the world (Gardner et al., 2018; Millan, 2019).

Prior to the advent of remote sensing, spatially distributed measurements of glacier flow velocities required lengthy field campaigns (Meier and Tangborn, 1965; Hooke et al., 1989; Chadwell, 1999; Mair et al., 2003). Nowadays full 2D flow-velocity maps may be readily calculated from a variety of optical and radar-based satellite imagery (Heid and Kääb, 2012b; Fahnestock et al., 2016). For this toolbox we focus on optical imagery products due to their ease of access, limited need for pre-processing and high spatial and temporal resolution (Drusch et al., 2012; Heid and Kääb, 2012b, a; Kääb et al., 2016; Darji et al., 2018).

A number of tools exist to derive displacements from imagery, as partially reviewed by Heid and Kääb (2012a); Jawak et al. (2018) and Darji et al. (2018). In addition, ~~near-global ice velocity~~ near-global ice-velocity maps are calculated in near-real time from Landsat and other freely available satellite data sources (Scambos, 2016; Gardner et al., 2020). Table 1 presents a

non-exhaustive list of software packages available online. Our objective with the 'Glacier Image Velocimetry' (GIV) toolbox presented here is to provide an ~~easy-to-use~~easy-to-use, flexible, and efficient tool that can ~~be used to~~ derive high spatial resolution and monthly temporal resolution surface-velocity maps of any glacier. The following section will run through the basics of ~~image feature tracking~~ the image-feature-tracking techniques and advances built into GIV.

2 Methods and model setup

The fundamental idea ~~of~~ behind feature tracking is based on techniques used to co-register images: the properties of two images are compared in order to identify the best-fit location of one image within the other (Scambos et al., 1992; Thielicke and Stamhuis, 2014; Messerli and Grinsted, 2015). In feature tracking, including in GIV, individual images are ~~broken down~~ divided into a grid of smaller images (referred to as 'chips'). We compare each individual 'chip' from the first image (I1) to the corresponding portion within a second image (I2), and find the best matching portion of I2. If no displacement has occurred between the two images, the best-fitting portion of I2 will have the same location as the original 'chip' on I1 (excluding any georeferencing or distortion-related errors). However, if any motion has occurred between the two images, the corresponding best matching 'chip' within I2 will be displaced relative the original location within I1. We may then determine the bulk displacement in pixels between the original I1 'chip' and best match I2 'chip'. The correlation coefficients between the original chip and surrounding area within I2 are also calculated. This allows a Gaussian curve to be fit to this grid in order to determine the peak location at sub-pixel accuracy. Repeating this routine for every chip within the original image allows a fully distributed 2D surface velocity field to be derived.

When initially developed for use in laboratory-based fluid dynamics, the camera, lighting, and tracer-particle conditions were all closely constrained (Grant, 1997; Raffel et al., 2018). On glaciers, features change over time as crevasses open and close, snow drifts, and ablation exposes new surfaces. In addition, the satellite may acquire imagery from slightly different locations and angles with each pass, and lighting conditions depend strongly on the time of day and year, as well as local weather conditions (Berthier et al., 2005; Kääb et al., 2016). This complexity raises additional problems in the use of this technique for deriving glacier velocities, and makes it entirely unusable in some cases (e.g. images too far spaced in time ~~or flow too rapid for glacier surface~~ relative to the speed of the glacier surface for image pairs to retain any coherence). These problems, however, are not insurmountable, and can be mitigated though a combination of image pre-filtering, comparison between adjacent velocity maps, and outlier filtering. We also refer readers to chapters 2 and 4 of Altena (2018) for further discussion on these topics. The Glacier Image Velocimetry toolbox makes use of these approaches, with a particular emphasis on noise reduction in individual velocity maps through the use of large datasets. Figure 1 presents the overall model setup and order of operations.

2.1 Model pre-processing

Prior to running the feature-tracking algorithms, the images are first loaded into the workspace and filtered. The user interface will prompt the user to enter the coordinates of the images (minimum and maximum latitude and longitude), and to select

Table 1. Non-exhaustive list of codes and toolboxes that may be used for feature tracking, and associated references. 3 = fully available, 2 = available, but relies on commercial software, 1 = not available. A spreadsheet with download links is available in the supplementary material.

Toolbox	Source	Summary	Avaliability
Auto-RIFT	Gardner et al. (2018)	Python dense feature tracking package for calculating displacement from optical or radar imagery. Used for calculating the ITS_LIVE global velocity dataset.	3
CARST	Zheng et al. (2019a)	Python and bash scripts for feature tracking and ice elevation change analysis.	3
CIAS	Kääb and Vollmer (2000)	IDL based correlation software to compute offsets between two images.	3
Cosi-Corr	Leprince et al. (2007a)	IDL/ENVI based package for image co-registration and displacement mapping.	2
EMT	Schwalbe and Maas (2017)	Workflow for analysis and feature tracking of tim -lapse ground based imagery.	3
GIV	This study.	GUI based feature tracking toolbox for glaciology	3
fourDvel	Minchew et al. (2017)	Fortran routine for calculation of 3d velocity fields from geolocated displacement data.	3
ImCorr	Scambos et al. (1992)	C and Fortran package for dense feature tracking of satellite or airphoto imagery.	3
ImGRAFT	Messerli and Grinsted (2015)	MATLAB based package for georectification of ground-based imagery and feature tracking.	2
matpiv	Sveen (2004)	MATLAB based toolbox for pattern matching and particle image velocimetry (PIV).	2
PIVlab	Thielicke and Stamhuis (2014)	GUI based MATLAB PIV toolbox	2
Pointcatcher	James et al. (2016)	MATLAB based toolbox for facilitating manual feature tracking in image time-series.	2
PyCorr	Fahnestock et al. (2016)	Python based feature tracking toolbox. Used for calculating the GoLIVE global velocity dataset.	1
PyTrx	How et al. (2020)	Python toolbox created for calculating displacements from oblique images and time-lapse image series.	3
SendIT	Nagy et al. (2019)	Flexible processing toolbox for retrieval of glacier surface velocities, based on ImCorr.	3
vmap	Shean (2019)	Ames Stereo Pipeline based image correlator for velocity map generation.	3

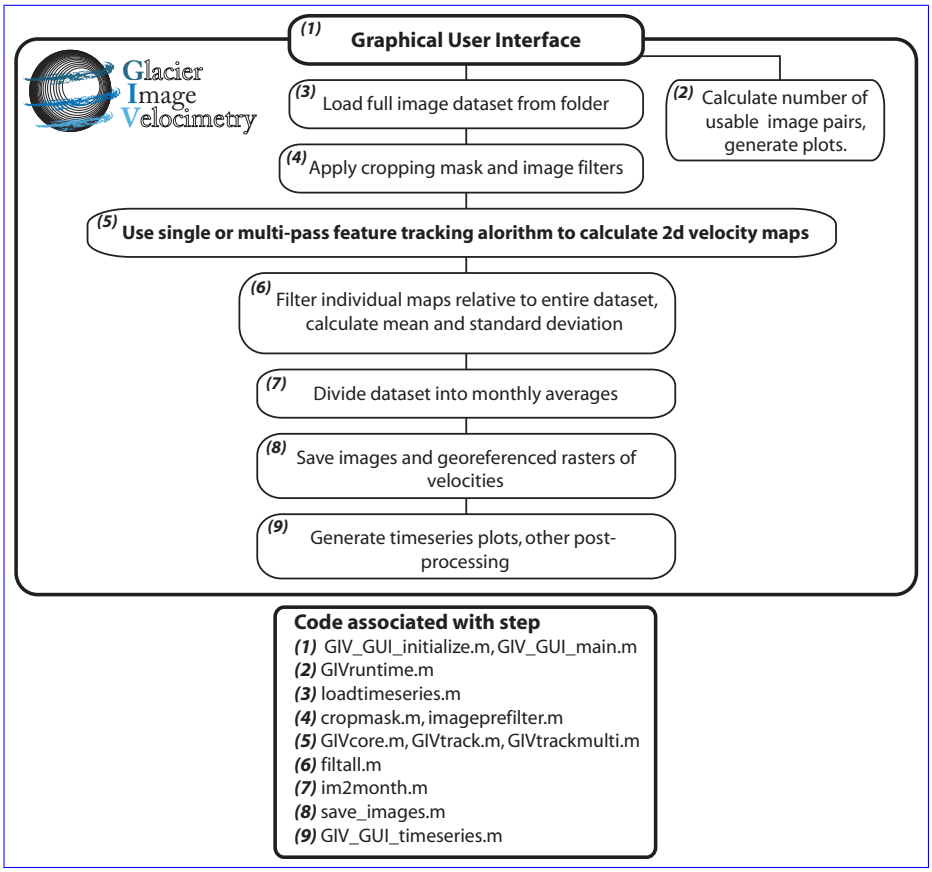

Figure 1. Flowchart describing the Glacier Image Velocimetry toolbox design. Names of the code files associated with each step are given for reference (and are available in the linked Zenodo repository). Note that users can access the source code, but that it is not necessary for running GIV. Users may enter all parameters into fields in the user interface~~. All~~ , with subsequent steps ~~are~~ automatically performed by the toolbox.

a given folder in which the images are stored. These images ~~must~~ can be .png~~or .jpg~~, .jpg, or .geotiff files of the area, with each file name being the date of image acquisition (in yyyymmdd format). ~~GIV will~~ In the case of a geotiff input, GIV will automatically load the geographic information from the input. GIV will then extract the dates from the file names, calculate time between images, and load the raw image data into an array for further processing. The user also inputs a modified image with glaciers of interest converted to pure white (RGB 255,255,255). This image is loaded by GIV and converted into a binary mask with areas within (1) and outside (0) the computational region. The size and resolution of images are also automatically calculated and resampled to a common resolution, such that images from different satellites may be combined into the same dataset.

Following this, GIV filters the images following user-defined settings. GIV includes a range of filters in order to reduce the effect of unwanted noise (e.g. clouds and shadows) and emphasize trackable features (e.g. crevasses, snowdrifts, supraglacial

debris). In particular we include high-pass, Sobel, and Laplacian filter options to emphasize short-wavelength features and edges, as well as intensity-capping and contrast-limited histogram-equalization filters to improve image contrast (Sveen, 2004; Thielicke and Stamhuis, 2014; Gardner et al., 2018). We also developed a 'near anisotropic orientation filter' (NAOF), which in most cases produces the highest number of correctly tracked velocity 'chips'. We define this filter as:

$$I_f = \sum_{\alpha} \mathrm{Re}\left[\exp\left(i \times \arctan 2(I_o * \alpha, I_o * R[\alpha]\right]\right) \tag{1}$$

With I_f the filtered image, I_o the original image, α representing four different convolution matrices oriented at 45 degrees from each other using the 8 adjacent pixels, $\mathrm{Re}[x]$ representing the real portion of complex number x, $\arctan 2(x, y)$ representing the four-quadrant arctangent (also called the two-argument arctangent), $x * y$ representing a two dimensional matrix convolution, and $R[x]$ representing a 90 degree matrix rotation. This filter works by summing differently angled orientation filters together in order to recover a 'pseudo-feature' with the same location as the original feature, but with an increased contrast between the feature and the background, and homogenized magnitude (Fitch et al., 2002; Kobayashi and Otsu, 2008). Information on absolute pixel color magnitude is discarded, with only information on color gradients preserved. A similar result may be obtained by convolving the original image with a single symmetrical convolution matrix, but this also normalizes all features to a single magnitude and results in a larger number of false matches. The NAOF ~~filter~~ has the advantages of (a) strongly increasing the contrast between features and background; (b) removing contrast differences between clouded, shadowed, and clear areas; and (c) preserving feature uniqueness. Figure 2 shows examples of how this filter is able to recover features from otherwise unusable images. Many glaciated areas remain partially cloud covered and shadowed for much of the year, so being able to recover partial velocity fields from these images can greatly increase the size of potential datasets. Note that no amount of filtering can improve certain images, such as those in which cloud cover is too thick for the surface to be visible.

2.2 Velocity calculations

Two main methods exist to derive displacements from an image pair. The first involves only a single pass across the images, and the second involves multiple passes with gradually reducing window sizes ~~(Raffel et al., 2018; Thielicke and Stamhuis, 2014)~~ (Thielicke and Stamhuis, 2014; Raffel et al., 2018). Single-pass methods generally have the advantage of generally being faster at coarse resolutions and are less at risk of smearing one erroneous value over a larger area. Multi-pass methods ~~on the other hand~~ update displacement estimates over multiple iterations, refining initial coarse-window-size displacement calculations using progressively smaller window sizes. Multi-pass methods combine the advantages of better feature matching at large window sizes with the higher spatial resolution of small window sizes. Both methods are integrated into GIV~~. The~~, whose single-pass method is based on a function from ImGRAFT (Messerli and Grinsted, 2015) and ~~the multipass method was edited~~ whose which uses a 3-iteration multi-pass algorithm was modified based on the matpiv toolbox (Sveen, 2004). Both functions have been tested in a number of previous studies, with matpiv being used extensively in fluid-dynamics research

~~(e.g., Lee et al., 2017; Oertel and Süfke, 2020; Sveen and Cowen, 2004; Sveen, 2004)~~(e.g., Sveen and Cowen, 2004; Sveen, 2004; Lee et a

.

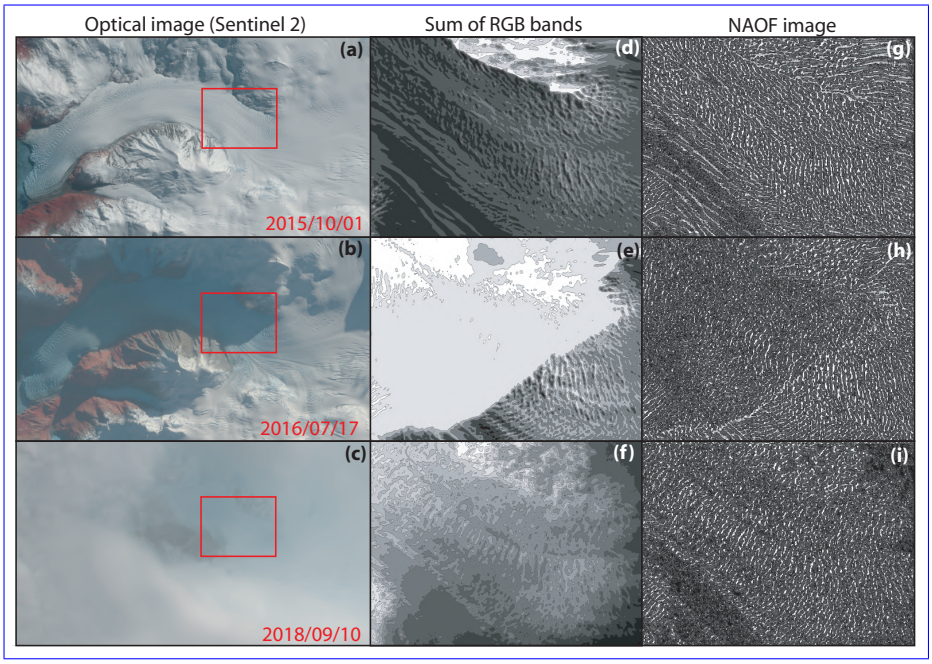

Figure 2. Comparison between raw optical images, ~~band summed~~ band-summed images and ~~NAOF filtered~~ NAOF-filtered images for a clear image (a, d, g), a heavily shadowed image (b, e, h), and a cloudy image (c, f, i). Note how despite the complexity, the NAOF images recover a clear and easily traceable feature pattern on the surface of the glacier that is suitable for obtaining velocities. The shadow line leaves an artefact in h, but is a marked improvement on the lack of features in the shaded area in e. Images from Sentinel-2.

The core of both the ~~single and multipass~~ single- and multi-pass methods involves converting each image chip to the frequency domain using a fast Fourier transform (FFT) algorithm, calculating the correlation coefficient with surrounding areas within a given search window, and converting the resulting similarity matrix back to the spatial domain with an inverse FFT (IFFT). This step is repeated on each chip within the original image, and is the most computationally expensive of the entire process.

GIV is written in MATLAB. Despite being a high-level interpreted programming language, MATLAB performs FFT calculations using precompiled C and Fortran bindings for the FFTW library ~~(Frigo and Johnson, 2005, 1998)~~(Frigo and Johnson, 1998, 2005) . Due to this being the rate-limiting step in feature tracking calculations (>90% of computation time in most cases), such code may be written in MATLAB with few performance issues relative to other programming languages.

Chip matching may also be performed in the spatial domain, where it is known as 'normalized' cross correlation. Spatial domain matching may better account for shear or distortion of features, but loses the computational efficiency of frequency-domain matches. We implement frequency-domain matching in GIV, as feature distortion is minimal in most glaciers. We refer readers to Thielicke and Stamhuis (2014) and chapter 4 of Altena (2018) for more details.

As the feature-tracking correlation between two images inherently requires a large number of FFT and IFFT operations, this step has limited potential for further optimization. Computation time may instead be decreased by deriving displacement fields from different image pairs in parallel rather than in series. This requires a slightly different code design: First, GIV detects the number of physical cores on the user's computer and starts a parallel pool (users may also start their own parallel pool with a chosen number of cores). It then decomposes the full sequence of image pairs into sub-sequences the size of the number of cores. Finally, it distributes each sub-sequence across the cores in the computer to be computed in parallel. Figure 3 shows the increase in computation speed with number of cores used in different scenarios. This enables large datasets to be processed more rapidly, even on standard laptop and desktop computers.

GIV may also calculate velocity maps for pairs of non-consecutive images, which we refer to as "temporal oversampling", resulting in much larger final datasets. The user inputs maximum and minimum temporal separations for image pairs, and GIV extracts all suitable pairs, including those that are not consecutive. For a dataset of ~~n~~ n images, this theoretically enables a total of ~~(n2-n)/2 image pairs(or~~ $(n^2 - n)/2$ image pairs. (For example, this would produce 19,900 image pairs ~~for a 200 satellite image~~ from a 200-satellite-image time-series). For heavily clouded datasets this also has the advantage of increasing the likelihood of forming cloud-free image pairs.

Apart from some scenarios and positions such as surges, spring speedups, and the margins of ice streams, glacier velocity gradients vary gradually in both space (low lateral velocity gradients) and time (low acceleration). Therefore, the accuracy of individual velocity measurements can be evaluated by comparing them to their immediate neighbours in both space and time. Sudden jumps in either most likely represent erroneous velocities due to mismatches within the feature-tracking algorithm. This property is used in the GIV toolbox to improve the final velocity maps through the following workflow:

Firstly, GIV filters each individual velocity map through user-prescribed limits on velocity and flow direction, as well as outlier detection functions. This finds values that differ by more than 50% from their immediate neighbours (4 surrounding cells) and 200% from the mean of their larger local area (25 surrounding cells), removes these outlier values, and interpolates across these now-empty pixels using the remaining values. Secondly, GIV calculates the mean, standard deviation, median, minimum, and maximum velocities ~~across the full~~ through time at each grid cell in the dataset. It then compares each individual value to the mean value at that location for the entire dataset. Any values more than 1.5 standard deviations away from this mean are considered outliers. This process is carried out both for the velocity and flow-direction grids, and only values within the threshold for both velocity and flow direction are conserved. This provides an additional check, as erroneous values are unlikely to coincidentally match both the velocity and flow direction. Finally, the entire dataset may be smoothed and interpolated in space and/or time and space according to the user's choices. This allows missing values at one timestep to be infilled from neighbouring times if the dataset is smooth enough to allow it. In addition, the displacement of each image pair may be normalized to the displacement of ~~user defined~~ user-defined stable ground to correct for systematic georeferencing errors.

Variable satellite repeat intervals and the exclusion of entirely clouded or otherwise unusable images lead to unevenly spaced velocity timeseries that are more difficult to interpret. In order to reduce this challenge, GIV includes a function that automatically averages the data and resamples it to monthly intervals. This is easy when all individual velocity maps cover periods of less than one month and do not overlap between months, but becomes more complex when they do. In many cases,

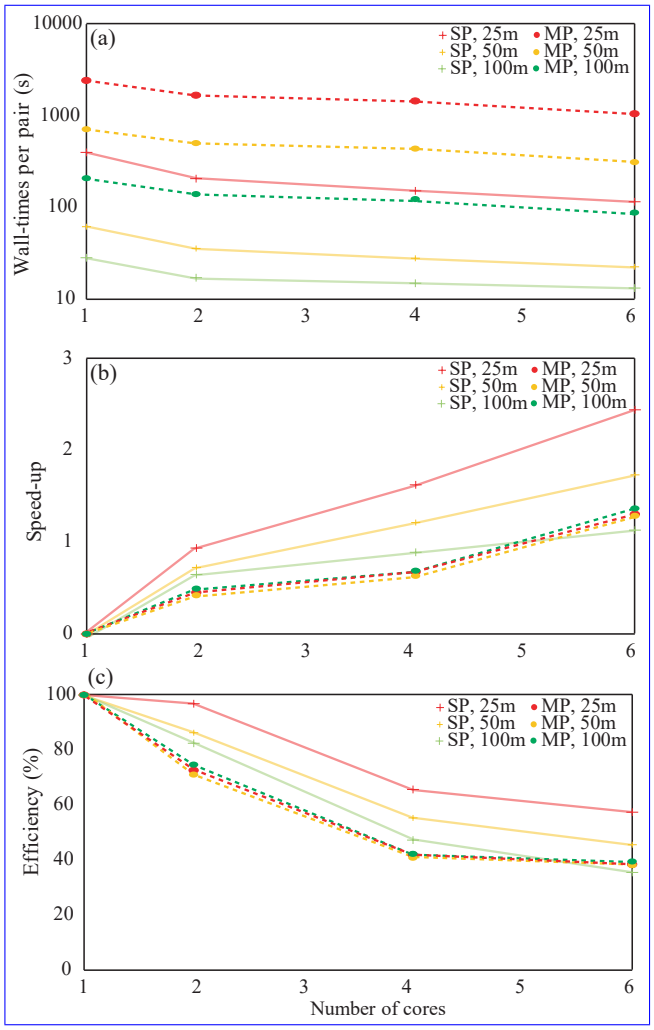

Figure 3. MP = Multi-pass; SP = Single-pass. Test conducted on a 12-image dataset of 10-m resolution, 1.7 million pixel images of Amalia Glacier, Chile using a Dell XPS 15 laptop (2×16GB DDR4 2666 MHz memory, 6-core Intel i7-8750H 2.20 GHz processor). In all cases, parallelization decreases runtime, and going from one to two cores improves runtime by 1.4–1.9×. Fine-resolution multi-pass runs usually yield the best velocity fields, and (b) shows that these benefit from the largest speed-up when parallelised.

image pairs with the shortest lag times (<7–10 days) are excluded because displacement over such a short time may be much smaller than offsets due to distortion and/or georeferencing errors. For the slowest-moving glaciers, this lower bound may be extended to several weeks or months. Lag times as long as the available imagery time series may be used so long as the surface of the glacier retains coherence in the image pairs.

185 GIV can determine monthly values by averaging across all image pairs that overlap with a given month. However, this will likely produce an artificially smoothed dataset due to the influence of velocities measured across the boundaries of months.

In order to make use of longer lag-time pairs, we develop an iterative strategy for calculating monthly values. In the first place, GIV takes a weighted mean of all velocities covering that month to make an initial guess at monthly velocities. The weighting parameter is determined by the proportion of the individual map contained within the given month, so for instance a velocity entirely within one month will be weighted 1 and one spread evenly over four months will be weighted 0.25. This initial estimate is then used to iterate between monthly averages and raw data values, with raw values covering more than one month split into monthly values by subtracting the previous iteration's estimate of monthly averages from them (Figure 4). This procedure may extract average monthly velocities even for months lacking any data. Outlier detection and maximum velocity filters are implemented to prevent small errors in the raw data from being accentuated by the iterations, but this may also lead to loss of data if too large a proportion of the initial dataset is inaccurate. Due to this limitation, the iterative calculations may not be adapted to some noisy datasets, for which the loss of temporal resolution by simple averaging will be preferable. Monthly averaging is performed as a post-processing step, and so may be repeated without the need to recalculate any raw velocity maps. Time series may also be generated from the raw data if monthly averaging is not desirable.

As a final step, GIV will automatically georeference the velocity grids and save ~~.tif~~ geotiff files to the user's computer. The toolbox also contains mapping tools that allow automatic generation of publication-quality images of the velocity and flow-direction maps (figure 5). In the following section we will examine some case studies of real glaciers and scenarios for which this model may be useful.

3 Results and Examples

Ice-velocity measurements supply essential information for studies of glacier dynamics, thickness, subglacial hydrology, and mass balance. With its GUI-based inputs and potential for parallelization, GIV can calculate a monthly velocity field for any glacier around the world with only a few hours of work. As such, it may also be run alongside field-based expeditions in order to understand the current conditions of the glacier and aid in instrumentation positioning.

We present four case studies. The first is of Glaciar Perito Moreno ~~,~~ (50.48°S, 73.11°W), where we use GIV to determine the displacement of automated ablation stakes in conjunction with fieldwork in Spring 2020. The second is Glacier d'Argentiere ~~,~~ (45.95°N, 06.97°E), a small and well-studied valley glacier located in the French Alps. The third is the Vavilov ice cap ~~,~~ (79.32°N, 94.34°E), located on October Revolution Island, in the Arctic Ocean off the mainland Russian coast, whose western outlet glacier is now surging into the ocean. ~~We validate PIV~~ Here we validate GIV against published results (Zheng et al., 2019b) using another image-based ice-velocity tool, CARST (Zheng et al., 2019a). Finally, we compute ice-flow velocities across the Chimborazo ice cap ~~in Ecuador, and use these to invert for ice thickness~~(01.45°S, 78.82°W) in Ecuador.

3.1 Field-campaign support: Glaciar Perito Moreno and the Southern Patagonian Icefield

A team from the University of Minnesota installed 3 automated weather stations and 3 automated ablation stakes near the southern flank of Glaciar Perito Moreno in order to better understand the local conditions of this glacier and construct temperature-index and energy-balance models for glacier ablation. We installed the automated ablation stakes, based off of designs by

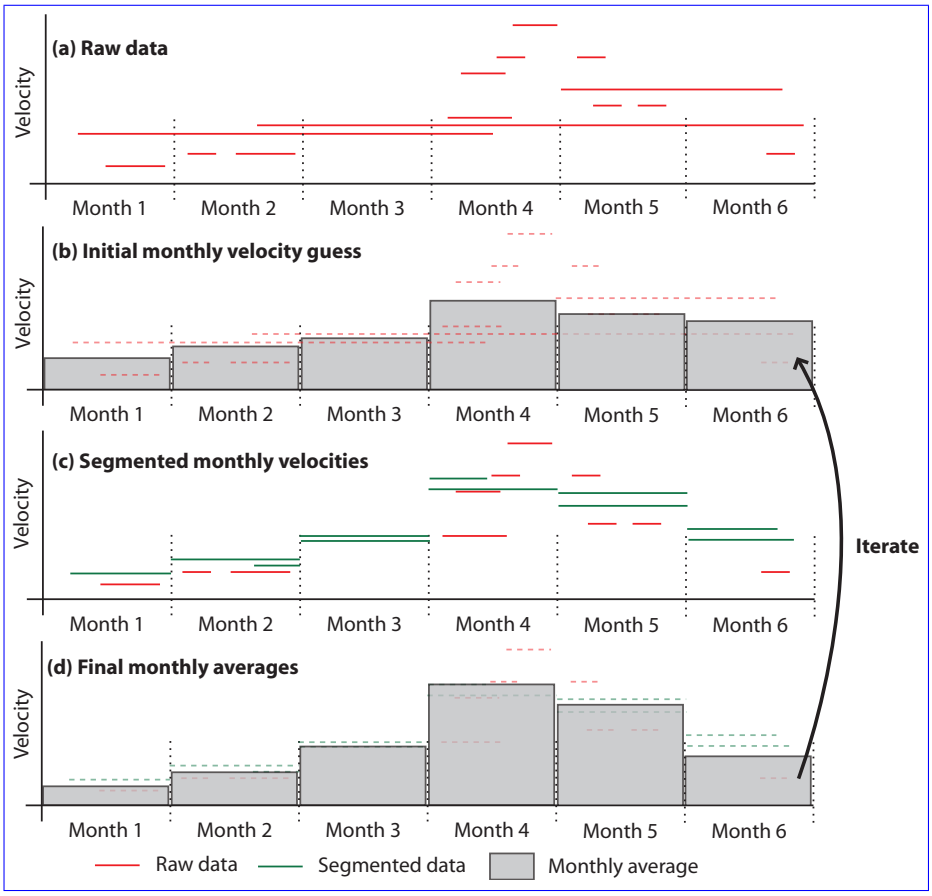

Figure 4. Schematic description of the techniques used to derive monthly velocities. The raw data (a) are combined in a weighted average to make an initial guess of monthly averages (b). The monthly averages are then used to segment longer time period velocity maps into their different monthly contributions (c). These are used to recalculate the monthly averages (d). Finally, GIV iterates over steps b–d for a number of times (e.g. 10) provided by user inputs. Note that an estimate may be made for the average velocity in 'Month 3', despite this month having no imagery available.

Wickert (2014) and Wickert et al. (2019), and tested by Saberi et al. (2019) and Armstrong and Anderson (2020), for 20 days between the 23rd of February and 14th of March, 2020. In slowly flowing glaciers, ice flow may be largely neglected when considering equipment recovery. In rapidly flowing glaciers such as Perito Moreno, however it may be relevant to consider the movement of the glacier when planning equipment recovery. This is particularly relevant where intense crevassing makes both access and visibility difficult. Figure 6 shows how different positioning decisions may influence ease of recovery: ablation stakes installed in position PM1 will move tens of metres towards the centre of the glacier in less than a month, whereas stakes in position PM3 will move less than 5 m towards the glacier flank. In our survey, stakes were installed around position PM3 for ease of access.

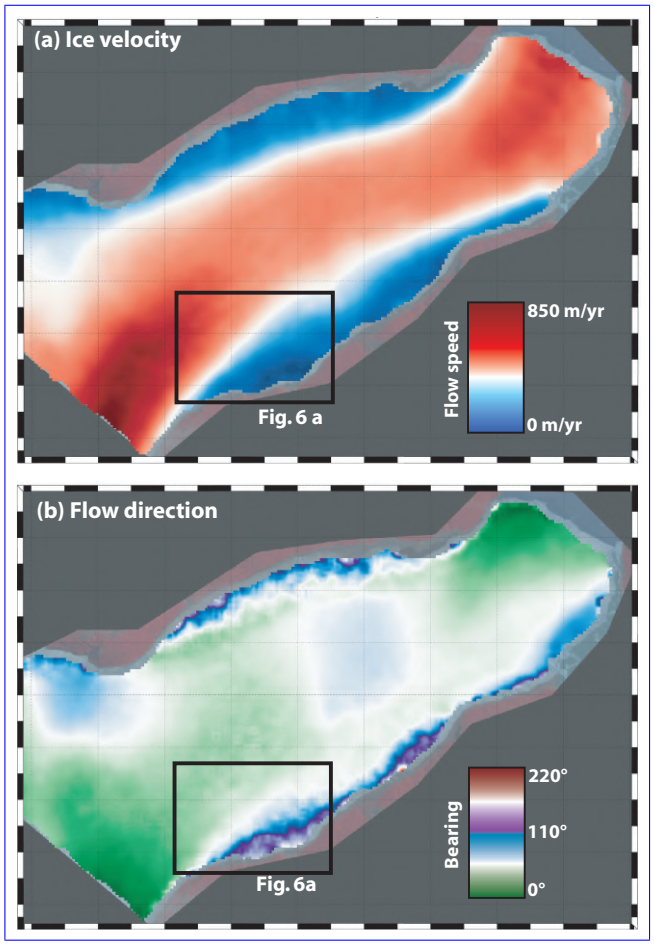

Figure 5. Mean flow velocity (m per year) (a) and direction (degrees) (b) of Glaciar Perito Moreno, Argentina for the first three months of 2020. Figure panels automatically generated from GIV, labels have been added and the color bars moved.

Figure 6 (b) also presents the case of Glaciar Europa, which drains the adjacent portion of the Southern Patagonian Icefield in Chile. We also derived the mean velocity field of this glacier over the past 3 years using Sentinel-2 imagery (195 image pairs). GIV velocity measurements reveal that the central portion of Glaciar Europa at its outlet flows nearly 10,000 $\mathrm{m/yr}$. If an ablation stake were installed in this area (point EU1), it would be displaced almost half a kilometre over the course of a 20-day survey. If it were instead placed at an alternative location 1 km to the West (EU2) it will be displaced only 20 metres in the same time period. This is an extreme case, and the flow speeds of most glaciers are orders of magnitude slower, but nonetheless reflects a situation in which deriving velocity fields would aid the success of a glaciological field campaign.

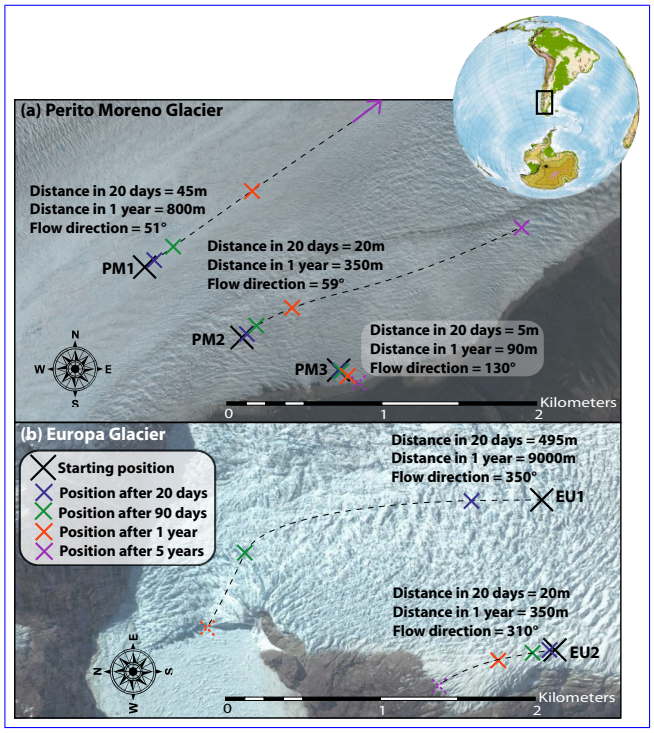

Figure 6. (a) Position of a point on Glaciar Perito Moreno with time for three different starting locations within 2 km of the glacier's southern margin. At PM1, ice speeds reach 800 m/yr and any equipment will be rapidly displaced. At PM3 ice-flow speeds are < 100 m per year and oriented towards the valley edge. (b) Identical plot for two points on Glaciar Europa. Any equipment installed at EU1 will be displaced several kilometres and lost to calving in less than 6 months. Imagery © Google Earth.

3.2 Valley-glacier velocity distribution: Glacier d'Argentière

In order to evaluate the effectiveness of GIV on smaller glaciers, we calculate a velocity field for a well-studied valley glacier in the Mont Blanc massif, Glacier d'Argentière (Benoit et al., 2015). We download one year worth of Sentinel-2 data (March 2019 – March 2020), containing over 1000 image pairs. These images are then used to derive a 25-m resolution mean-ice-velocity map, shown in Figure 7. The sparsity of features transverse to flow direction on Glacier d'Argentière make it difficult for feature-tracking methods to calculate velocities. Nevertheless, the resulting flow-velocity map is comparable to those derived using a SPOT satellite image pair from 2003 (Berthier et al., 2005; Rabatel et al., 2018), SAR and ground based photogrammetry (Benoit et al., 2015), and a different feature-tracking routine based on a modified version of ampcor (Millan et al., 2019). The velocity map highlights accelerated ice flow at the terminus icefall and on the steep tributary glacier to the SW of the main trunk (Figure 7). Main-trunk velocities are on the order of 45–70 $\mathrm{m/yr}$, slightly slower than Berthier et al. (2005)'s SPOT values but in line with Benoit et al. (2015)'s values. Our values represent the mean over an entire year, including the slower

winter velocities captured by Berthier et al. (2005). It is also possible that glacier thinning has reduced its flow velocity, but sufficient data to evaluate this do not exist.

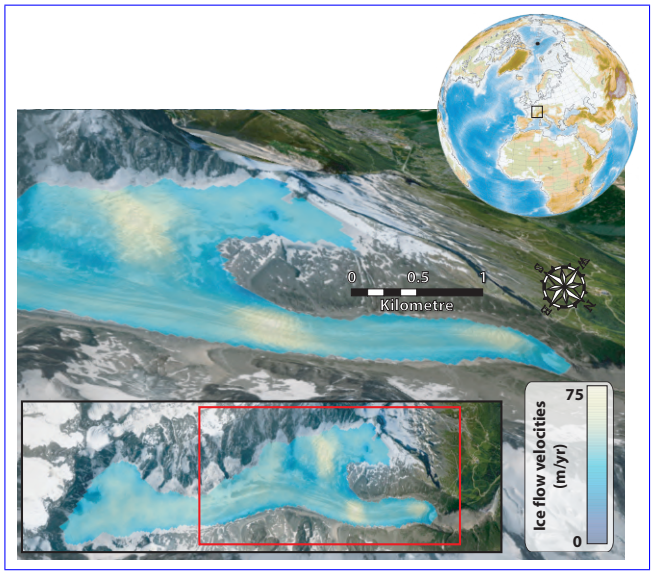

Figure 7. Perspective view of mean flow velocities of Glacier d'Argentière, France over the period 03/2019–03/2020. Imagery © Google Earth, scale for near margin of glacier.

3.3 Validating GIV by observing Vavilov ice cap dynamics

3.3.1 Mapping ice surge

Arctic land-ice melt has contributed more than 20 mm to global sea level rise since the 1970s (Box et al., 2018). Most of these large glaciers and ice caps remain remote and difficult to access, and high spatial and temporal resolution surface velocity maps provide one important tool to assess their response to changing environmental conditions.

The Vavilov ice cap is a 1700 km^3 ice cap located on October Revolution Island in the Severnaya Zemlya archipelago, located in the Russian high arctic (Bassford et al., 2006). Until the 2010s, the Vavilov ice cap exhibited surface velocities of only a few tens of metres per year, typical of many cold-based high-arctic ice masses. In 2013, a large portion of the marine-terminating western flank surged, with the ice front reaching more than 10 km beyond its prior grounding line by 2016 (Willis et al., 2018; Zheng et al., 2019b). This sudden shift in ice behaviour was not accompanied by any dramatic climatic shift, and the exact triggers are a matter of active debate (Willis et al., 2018, and references therein). Willis et al. (2018) proposed that the dramatic acceleration is related to the ice cap overriding weak marine sediments in the Kara Sea, which can deform easily and substantially increase ice velocity. The ice cap margin is also no longer frozen to bedrock, leading to associated removal of resistive stresses at the ice front (Willis et al., 2018). Rapid ice flow initiates a set of internal feedbacks to further increase ice velocity, including strain softening of thie ice itself; shear heating that produces meltwater, capable of reducing the effective

normal stress of the ice and hence its friction against the bed; and potential infiltration of this water into the bed material, increasing its deformability (Willis et al., 2018, and references therein). With no direct data on subglacial conditions prior to or during the surge, the exact processes involved remain difficult to reveal. We may, however, monitor surface ice velocities to examine the ongoing changes in ice ~~dynamics~~kinematics.

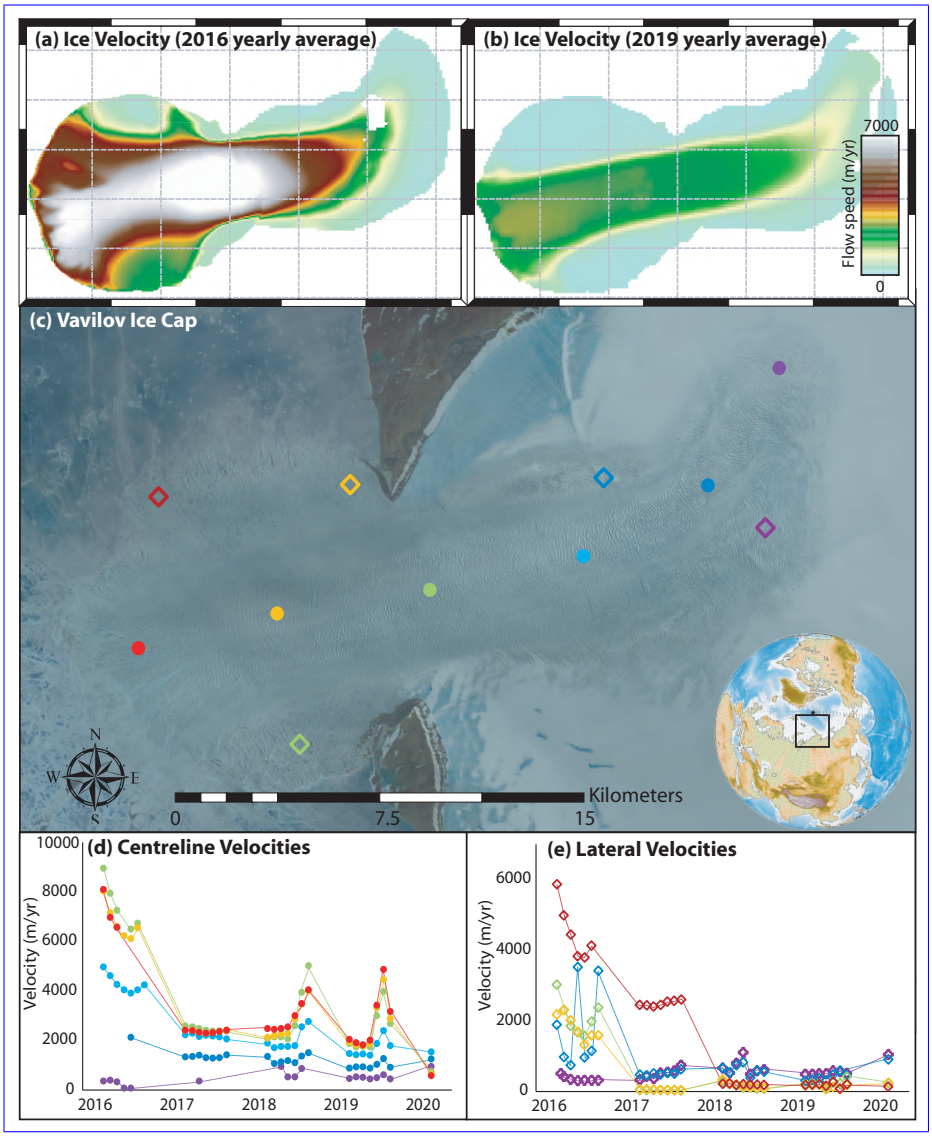

Figure 8. (a) and (b) present 100-m-resolution annual mean velocities for the western outlet glacier of the Vavilov ice cap. (c) displays a 2019 Sentinel-2 image showing the main features of this outlet and the locations used to derive monthly timeseries. (d) and (e) present monthly resolution velocity timeseries along the glacier centreline and flanks using Sentinel-2 imagery.

Visible-band imagery from the Vavilov ice cap is available only for summer months (March to September) due to darkness during the high-latitude boreal winter. We use GIV to derive a 100-m resolution ice-velocity map of a 365-km^2 area of the Western flank of the ice cap using the entire Sentinel-2 archive (beginning in 2016). Figure 8 (a) and (b) present two average yearly velocity maps for the apex of the surges in 2016 and 2019. Panels (d) and (e) present timeseries of monthly velocities over the period from March 2016 to March 2020 at the locations shown in figure 8(c).

Velocities of the centreline points converge over the time period considered: Although the velocities near the ice front decrease from the 2016 peak (red, orange, and green circles), velocities of regions most distant from the coast show a steady increase (purple points). The central portion of this newly formed outlet glacier shows distinct late-summer accelerations in both 2018 and 2019, reaching around double ~~the~~ its spring and early summer rates and rapidly decaying (figure 7(d)). Within the newly formed western frontal lobe, extruded beyond the prior grounding line, flow has concentrated into a single branch with well-developed shear margins separating a central region with rapid ice flow from slow-moving lateral portions of the glacier (Zheng et al., 2019b).

Extraction of high-resolution ice velocities in this region using GIV confirms Willis et al. (2018) and Zheng et al. (2019b)'s findings that the western portion of Vavilov has entered into a new fast-flow regime. The late summer velocity peaks in both 2018 and 2019 may shed some light on the driving forces behind this acceleration if associated changed in climatic, ice surface or ice basal conditions are identified. Ongoing monitoring will help to determine whether a similar peak occurs in 2020 or any following years, and can be performed in near real time using GIV.

3.3.2 Method validation

We compare our GIV-derived results against a velocity map of the front of the western outlet glacier generated by Zheng et al. (2019b) using CARST (Zheng et al., 2019a). Zheng et al. (2019b) ~~'s velocities were generated~~ generated their velocity map based on a single Landsat 8 pair dated 2017/05/06 and 2017/05/22. We compared the ice-surface velocity magnitude calculated from this pair to the May 2017 average velocity map generated from Sentinel-2 imagery using GIV through the approach described above. We georeferenced the two velocity maps using the glacier margins and other notable features. The difference map (Fig. 9(a)) displays the highest amplitude anomalies along the margins of the central high-velocity band. Differences between the GIV- and CARST-derived velocity maps are normally distributed, with a mean difference of -16 m per year (Fig 9(c)). This mean difference is $\leq$1% the speed across the majority of the glacier surface (Fig 9(b)). In this region of the glacier surface, the annual variability in ice-surface velocities is on the order of several hundred metres per year (Fig 8(d) and (e)), and this difference between our results using GIV and those of Zheng et al. (2019b) could plausibly result from the slightly different dates covered or differing image resolutions (10 m for Sentinel-2 compared to 15 or 30 m for Landsat). The high-magnitude difference bands on either side of the fast-moving central region may also result in whole or part from georeferencing errors in GIV, in CARST, or in our work to georeference these two velocity maps to one another.

3.4 ~~Ice-thickness inversions and~~ Ice-velocity of a small tropical ~~glaciers: Chimborazo~~ ice cap: Chimborazo

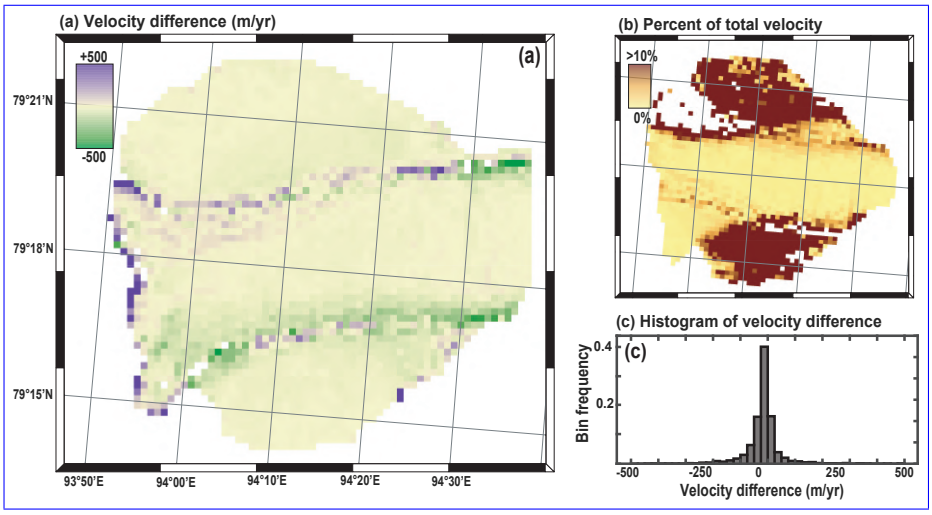

Figure 9. Comparison between Zheng et al. (2019b)'s velocity maps for Vavilov ice cap (Pair037_20170506_20170522) with results from GIV (May 2017 average). a) shows a difference map~~between the two results (~~, corresponding to Zheng et al. velocity minus GIV velocity~~)~~, b) shows what percentage of the total velocity this difference represents (absolute value of the difference shown in a) divided by GIV velocity), and c) is a histogram of the difference values. The mean difference between the two velocity maps is less than 20 m per year, or less than 1% of the total velocity for much of the area.

~~There are many glaciers for which ice thickness measurements would be useful, but traditional radar or borehole techniques are too challenging or expensive to apply. In these cases, we may combine our remotely derived ice-surface velocities with knowledge about ice-flow mechanics to estimate ice thickness and volume (Gantayat et al., 2014; Farinotti et al., 2019). Where no data are available, these approaches can provide a physics-based first estimate. Where even one or a few data points are available, these can help to calibrate ice-flow parameters and perform a physics-based extrapolation of local field measurements, resulting in a spatially distributed measure of ice thickness – and hence, volume.~~

Many tropical glaciers and ice caps have limited ~~or no ice-thickness information~~ to no ice-flow data (Thompson et al., 2011). These are important water sources to millions of people ~~(Bury et al., 2011; La Frenierre and Mark, 2017; Chevallier et al., 2011)~~ (Bury et al., 2011; Chevallier et al., 2011; La Frenierre and Mark, 2017). Vergara et al. (2007) estimated the economic cost of glacier retreat on water use to be in the hundreds of millions of U.S. dollars, and the impact on Peru's electrical utility to be ∼1.5 billion. ~~Accurate and spatially-distributed~~ High resolution estimates of ice ~~thickness can therefore support~~ velocity provide information on glacier state, and can contribute to practical decision making in the tropical Andes.

Chimborazo is a 6268 m high stratovolcano in Ecuador capped with an ice cap and 17 outlet glaciers. On Chimborazo's north-eastern flank, glacier meltwater drives nearly all of the discharge variability, and the disappearance of the prominent Reschreiter Glacier could decrease the discharge of the watershed's outlet stream by up to 50% (Saberi et al., 2019). Due to its high elevation and steep slopes that are unstable in regions of recent ice retreat, the glaciers on Chimborazo are difficult to survey (Saberi et al., 2019). ~~Ice cores have been collected at the summit plateau in 1999–2000, the longest of which extends~~

54.4 to the glacier bed (Schotterer et al., 2003; Ginot et al., 2010).The general data sparsity but existence of a single point for benchmarking, combined with its water-supply importance for the surrounding communities (La Frenierre and Mark, 2017), makes it an appropriate target for an initial ice-thickness inversion using GIV. No field measurements of glacier surface velocity have been conducted.

Ice surface velocity map for the Chimborazo ice cap calculated with GIV. Imagery © Google Earth and Sentinel-2.

3.4.1 Inverting surface velocity for ice thickness

Glacier motion occurs though a combination of internal deformation, basal sliding and subglacial sediment deformation. Ice flows under its own weight, and the rate of internal deformation is a function of the thickness of the ice. Ice-surface velocities $u(H)$ may be written as:

$$u(H) = u_{d,H} + u_s + u_t.$$

Here, the ice thickness H denotes that the velocity is evaluated at the ice surface , $u_{d,H}$ is the surface velocity produced by internal deformation alone, u_s is the rate of basal sliding, and u_t is the component of glacier velocity produced through till deformation.

We first work to remove terms from this expression. The glaciers on Chimborazo flow over bedrock, thus u_t should be at or near zero. Glacial sliding requires warm-based ice and can be enhanced by water pressure (e.g., MacGregor et al., 2000). Meltwater has been identified near the summit of Chimborazo, where coring attempts in December 2000 were disrupted by a layer of waterlogged ice at a depth of 28 (Schotterer et al., 2003). However, surface melt was exceptional in the years 1999–2000 due to tephra fallout from the nearby eruption of Tungurahua (Schotterer et al., 2003; Ginot et al., 2010). The 0°C isotherm was estimated at 5050 m using multiple field based temperature sensors (La Frenierre and Mark, 2017). This is consistent with a 0°C isotherm of 4922 m calculated from from two weather stations in the vicinity of Chimborazo (La Frenierre and Mark, 2017; Saberi et al., 2019): Boca Toma (W078.7508, S01.4482, elevation 3899 m) and Reschreiter camp (W078.7741, S01.4459, elevation 4355 m). This suggests that most or all of Chimborazo's ice cap is geographically above and thermally below the 0 degree isotherm, and therefore is composed of cold-based ice that cannot slide. As a result of the hard bed and mostly cold-based ice, we approximate that internal deformation alone sets glacier-surface velocity:

As a result of the hard bed and mostly cold-based ice, we approximate that internal deformation alone sets glacier-surface velocity:

$$u(H) = u_{d,H} = \frac{2A_c}{n+1}\tau_b^n H.$$

Here, τ_b is the basal shear stress, A_c is the Arrhenius creep constant, and n is Glen's flow exponent. Our use of the basal shear stress instead of the full driving stress for glacier motion comes from the shallow-ice approximation. Through this, we assume that local stresses induced by the ice are much greater than stresses induced lateral coupling between columns of ice. We next expand basal shear stress, τ_b, into measurable parameters:

$$\tau_b = f\rho_i g H \sin(\alpha).$$

Here, f is a shape factor accounting for lateral drag along glacier margins (Gantayat et al., 2014; Jiskoot, 2011; Linsbauer et al., 2012), ρ_i is the density of ice, g is gravitational acceleration, α is ice-surface slope angle, and H is ice thickness.

Combining equations **??** and **??** and rearranging them to solve for ice thickness, H, gives the following expression:

$$H = \left(\frac{n+1}{2A_c(f\rho_i g)^n}\right)^{1/(n+1)} \left(\frac{u(H)}{\sin(\alpha)^n}\right)^{1/(n+1)}.$$

Here, the first bracket contains defined parameters and the second bracket contains observations obtained from GIV ($u(H)$) and a digital elevation model ($\sin(\alpha)$). We use parameter values from Cuffey and Paterson (2010); Gantayat et al. (2014) and Haeberli and Hoelzle (1995): $A_c = 3.24 \times 10^{-24}$, n=3, f=0.9, $\rho_i = 917$ and $g = 9.79$. We compute ice-surface slope, α, from elevation data collected by the Shuttle Radar Topography Mission (SRTM GL1: Farr et al., 2007). The longitudinal coupling length is around one to three ice thicknesses in valley glaciers (Kamb and Echelmeyer, 1986), which is on the order of 150 at Chimborazo. To ensure that we provide results that are consistent with the shallow-ice approximation, we resample ice-surface slope derived from the Shuttle Radar Topography Mission data to a 150 resolution average. Thus, the only unknown required to solve for ice thickness, H, is ice-surface velocity.

Chimborazo poses challenges to feature-tracking-based ice velocimetry, as its glaciers are small, often feature-poor or snow-covered, very slow moving, and regularly cloud covered. The velocity limitations are mitigated by using only images with large temporal separation (acquisition dates more than six months apart). GIV is also well suited for extracting velocities from partially clouded imagery. We run GIV on the full Sentinel-2 dataset, which comprises 3090 image pairs with separation of more than of 91 individual partially or fully cloud-free images. These were cropped to Chimborazo, resulting in 3062 image pairs separated by at least six months. Resultant ice velocities for each pair were corrected for the mean displacement of a stable, non-glaciated region surrounding the ice cap. Results are shown in Figure 10. The runtime for this calculation is approximately 2 hours on a Dell XPS 15 laptop (2×16GB DDR4 2666 MHz memory, 6-core Intel i7-8750H 2.20 GHz processor). We then use Equation **??**, above, to compute a spatially distributed ice-thickness map for Chimborazo.

Figures 10 and **??** show the initial ice-velocity product and the final ice-thickness map (inversion code available online from Van Wyk de . Ice is thickest on the eastern outlet glaciers, consistent with higher precipitation on the eastern flank of Chimborazo (Saberi et al., 2019) . Ice is also thicker on the flat summit plateau where a 54.4 ice core was drilled to bedrock in 2000 (Ramirez et al., 2003; Schotterer et al., 20 , within 10% of the 60 ice thickness the model predicts in this location. If this velocity-based inversion is correct, it implies that the Chimborazo ice cap is thickening despite rising temperatures at an average rate of 0.11 per decade since the 1980s (La Frenierre and Mark, 2017), or around 0.2 since the summit ice core was drilled to bedrock. Ice-cap thickening could be explained by an increase in accumulation, as has been proposed for other South American glaciers (e.g. Warren et al., 1997) . A higher-than-expected modelled ice thickness could also be explained by uncertainties in the inversion parameters or by invalidities in the assumption of purely internal-deformation-driven surface velocity. A lower bulk ice density (ρ_i), Arrhenius creep constant (A_c) or Glen's flow law exponent (n) would also all lead to lower estimates of ice thickness.

Integrating the ice thickness over the entire area shows that Chimborazo's ice cap stores around 3.9×10^{8} ^{3} of ice, or just over a third of a cubic kilometre. Most of this ice volume is stored within the summit plateau and east-verging outlet glaciers, with little ice remaining in south- and west-facing outlet glaciers. This is less than half of Farinotti et al. (2019)'s estimate for the ice

~~volume at Chimborazo in the year 2000 (8.3×10^{8} ^{3}). Part of this difference is related to the larger glacier extent polygon from the year 2000 used by Farinotti et al. (2019) in their calculation. This ice polygon may incorrectly include snow covered bedrock, and represent an over-estimation of the ice extent in the year 2000 (e.g. La Frenierre and Mark, 2017). Farinotti et al. (2019) do not use any ice-velocity data, but use several inversion methods based on glacier geometry, topography, climate and ice thickness measurements. Figure ?? compares the ice-thickness map created by inverting GIV ice velocities and from Farinotti et al. (2019). They predict that ice was thickest (>100 thick) on the western flank of Chimborazo. The majority of this area is now entirely ice free, which would require ice thinning of up to 5 per year to reconcile with Farinotti et al. (2019)'s computed ice thicknesses.~~

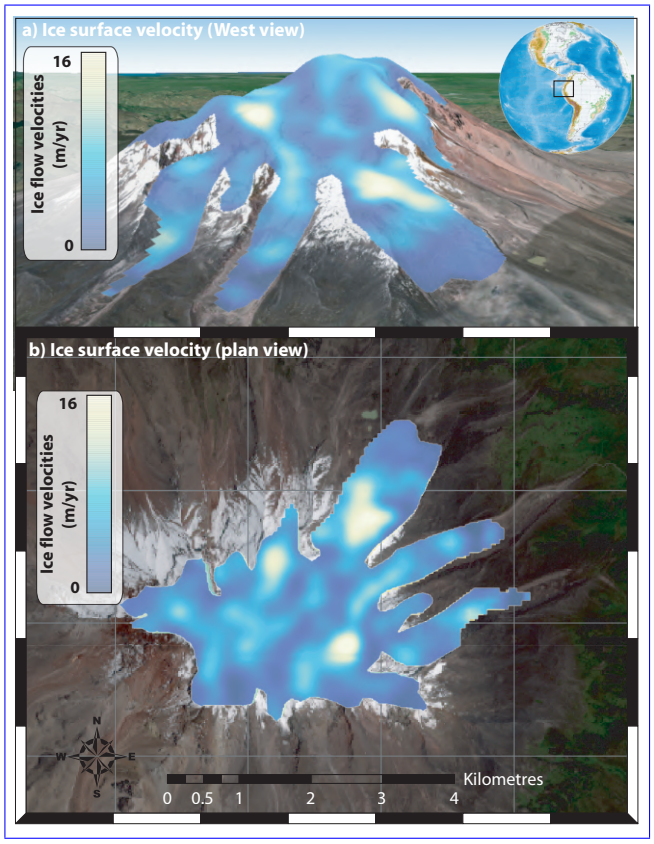

Figure 10. ~~Ice thickness~~ Ice-surface-velocity map for the Chimborazo ice cap ~~, Ecuador inverted from~~ calculated with GIV~~(a) and from Farinotti et al. (2019) (b). The cross labeled 'IC' marks the position an ice core was drilled at Cumbre Ventimilla in 2000, reaching bedrock at 54.4 m (Schotterer et al., 2003). Note Farinotti et al. (2019) estimate ice thicknesses of >100 in areas on the western flank that are now ice free.~~ Imagery ~~from~~ © Google Earth and Sentinel-2.

4 Discussion

These four examples underline the versatility of GIV for calculating ice velocities in diverse environments. GIV's usefulness derives from its flexibility, ease of use, and ability to rapidly process large datasets. Most regular laptop and desktop computers now include at least 4 cores, which GIV uses to speed up calculations by a factor of two or more (Figure 3). This makes velocity-field calculations with hundreds to thousands of image pairs possible on regular computers. The inclusion of 'temporal oversampling' allows much larger datasets to be generated than via simple consecutive-image comparison; a dataset of 100 images may in fact include several thousand usable image pairs. We combine methodological advances in feature tracking and image processing from both geoscience and engineering toolboxes, and develop new filtering techniques to improve the quality of the final surface-velocity maps. GIV provides a rapid and ~~easy to use~~ easy-to-use interface (shown in Figure 11) and a user manual, and may also be of use to communities who would not generally be involved with glacier remote sensing (Van Wyk de Vries, 2020a, b).

~~Other~~ Many other feature-tracking algorithms have been used in glaciological research. These include CARST (Cryosphere and Remote Sensing Toolkit: Willis et al., 2018), COSI-corr (Co-registration of Optically Sensed Images and Correlation: Leprince et al., 2007b), AutoRIFT (Autonomous Repeat Image Feature Tracking: Gardner et al., 2018), ImGRAFT (Image Georectification and , and SenDiT (the Sentinel-2 Displacement Toolbox: Nagy and Andreassen, 2019; Nagy et al., 2019). CARST contains a mixture of Python and Bash scripts used to monitor changes in glaciers, and includes feature-tracking and ice-elevation-change-monitoring tools ~~(Willis et al., 2018; Zheng et al., 2019a, 2018)~~(Willis et al., 2018; Zheng et al., 2018, 2019a). COSI-Corr is a flexible co-registration and feature-tracking tool written in IDL, implemented in the ENVI GIS package, and initially used for measuring co-seismic deformation. Auto-RIFT is a Python-based feature-tracking algorithm (Gardner et al., 2018) with similar core components to GIV. It was used to calculate yearly resolution average velocity maps of the Antarctic and Greenland ice sheets (ITS_LIVE dataset). ImGRAFT is a MATLAB-based toolbox for georectifying and feature-tracking of ground based imagery, and may also be used on satellite imagery. SenDiT provides a platform to automatically download and generate velocity maps based on Sentinel-2 data, using a Python interface with bindings to the ~~C and Fortran based~~ C- and Fortran-based *imcorr* toolbox (Scambos et al., 1992) for feature-tracking calculations.

In some circumstances, GIV will not be the most suitable feature tracking tool. For example, users ~~requiring prior~~ who need to manually perform prior image co-registration ~~of images~~ (e.g. with airphotos) may still wish to use COSI-Corr. The objective of GIV is not to compete with or replace all the above tools, but rather to provide an ~~easy to use, flexible~~easy-to-use, flexible, and robust alternative. GIV is ~~quick to learn and fast to run, and~~ easily learned and is not computationally time-consuming, and the results derived with it are easy to reproduce. GIV allows users to modify image-processing and feature-tracking parameters based on their expert knowledge of particular glaciers, without the need for specific computational knowledge. GIV may be run either directly through MATLAB functions, through a MATLAB graphical user interface (Van Wyk de Vries, 2020a), or as an independent desktop app that may be run with no MATLAB license (Van Wyk de Vries, 2020b). GIV has been tested and successfully run on Windows, Mac and Linux operating systems.

Figure 11. Main graphical user interface for GIV, showing the main input fields. This interface may either be run through MATLAB or as an independent desktop app with no licensing requirements.

5 Conclusions

GIV is a versatile, GUI-based, and fully parallelised toolbox that enables rapid calculation of glacier velocity fields from satellite imagery. GIV incorporates recent improvements in optical satellite imagery availability and resolution to extract high temporal and spatial resolution velocity maps, and uses novel and pre-existing filters to optimise the quality of these velocity maps. GIV has been successfully tested on a wide range of environments, including small valley glaciers (Glacier d'Argentière, France), tropical ice caps (Volcán Chimborazo, Ecuador), and large outlet glaciers (Glaciar Perito Moreno, Argentina, and outflow from the Vavilov Ice Cap, Russia). We show that ice-velocity datasets are versatile and may be used to compliment

field campaigns, ~~study glacier dynamics , and make ice-volume estimates~~and study the dynamics of large and small glaciers. Source code and pre-compiled binary executables for GIV are availble from Van Wyk de Vries (2020a) and Van Wyk de Vries (2020b).

Code availability. MATLAB code for GIV may be downloaded from https://github.com/MaxVWDV/glacier-image-velocimetry (Van Wyk de Vries, 2020a). The GIV standalone app may be downloaded from https://github.com/MaxVWDV/glacier-image-velocimetry-app (Van Wyk de Vries, 2020b). Both include a user manual and examples.

Author contributions. MV and AW planned the project. MV wrote the code and ran the examples. MV and AW wrote and edited the manuscript.

Competing interests. The authors declare no competing interests.

Acknowledgements. MV was supported by a University of Minnesota College of Science and Engineering fellowship. Ben Popken assisted with early testing of GIV. Emi Ito, Kelly MacGregor, Jeff La Frenierre, Matias Romero, Shanti B. Penprase, Jabari Jones and Kerry L. Callaghan provided comments on this manuscript. We thank Ted Scambos and an anonymous reviewer for thoughtful reviews, which improved both the manuscript and associated toolbox. We further acknowledge editor Harry Zekollari for providing welcome feedback and suggestions. This material is based upon work supported by the National Science Foundation under Grant No. EAR-1714614, coordinated by Lead PI Maria Beatrice Magnani.

References

AghaKouchak, A., Farahmand, A., Melton, F. S., Teixeira, J., Anderson, M. C., Wardlow, B. D., and Hain, C. R.: Remote sensing of drought: Progress, challenges and opportunities, Reviews of Geophysics, 53, 452–480, https://doi.org/10.1002/2014RG000456, http://agupubs.onlinelibrary.wiley.com/doi/abs/10.1002/2014RG000456, _eprint: https://onlinelibrary.wiley.com/doi/pdf/10.1002/2014RG000456, 2015.

Altena, B.: Observing change in glacier flow by using optical satellites, https://www.duo.uio.no/handle/10852/61747, accepted: 2018-05-28T11:09:27Z, 2018.

Armstrong, W. H. and Anderson, R. S.: Ice-marginal lake hydrology and the seasonal dynamical evolution of Kennicott Glacier, Alaska, Journal of Glaciology, pp. 1–15, publisher: Cambridge University Press, 2020.

Bakke, J. and Nesje, A.: Equilibrium-Line Altitude (ELA), in: Encyclopedia of Snow, Ice and Glaciers, edited by Singh, V. P., Singh, P., and Haritashya, U. K., pp. 268–277, Springer Netherlands, Dordrecht, https://doi.org/10.1007/978-90-481-2642-2_140, https://doi.org/10.1007/978-90-481-2642-2_140, 2011.

Bamber, J. L. and Rivera, A.: A review of remote sensing methods for glacier mass balance determination, Global and Planetary Change, 59, 138–148, https://doi.org/10.1016/j.gloplacha.2006.11.031, http://www.sciencedirect.com/science/article/pii/S0921818106003055, 2007.

Bassford, R. P., Siegert, M. J., Dowdeswell, J. A., Oerlemans, J., Glazovsky, A. F., and Macheret, Y. Y.: Quantifying the Mass Balance of Ice Caps on Severnaya Zemlya, Russian High Arctic. I: Climate and Mass Balance of the Vavilov Ice Cap, Arctic, Antarctic, and Alpine Research, 38, 1–12, https://doi.org/10.1657/1523-0430(2006)038[0001:QTMBOI]2.0.CO;2, https://www.tandfonline.com/doi/abs/10.1657/1523-0430%282006%29038%5B0001%3AQTMBOI%5D2.0.CO%3B2, publisher: Taylor & Francis _eprint: https://www.tandfonline.com/doi/pdf/10.1657/1523-0430%282006%29038%5B0001%3AQTMBOI%5D2.0.CO%3B2, 2006.

Benoit, L., Dehecq, A., Pham, H.-T., Vernier, F., Trouvé, E., Moreau, L., Martin, O., Thom, C., Pierrot-Deseilligny, M., and Briole, P.: Multi-method monitoring of Glacier d'Argentière dynamics, Annals of Glaciology, 56, 118–128, https://doi.org/10.3189/2015AoG70A985, https://www.cambridge.org/core/product/identifier/S0260305500250398/type/journal_article, 2015.

Berthier, E., Vadon, H., Baratoux, D., Arnaud, Y., Vincent, C., Feigl, K. L., Rémy, F., and Legrésy, B.: Surface motion of mountain glaciers derived from satellite optical imagery, Remote Sensing of Environment, 95, 14–28, https://doi.org/10.1016/j.rse.2004.11.005, http://www.sciencedirect.com/science/article/pii/S0034425704003463, 2005.

Bindschadler, R., Vornberger, P., Fleming, A., Fox, A., Mullins, J., Binnie, D., Paulsen, S. J., Granneman, B., and Gorodetzky, D.: The Landsat Image Mosaic of Antarctica, Remote Sensing of Environment, 112, 4214–4226, https://doi.org/10.1016/j.rse.2008.07.006, http://www.sciencedirect.com/science/article/pii/S003442570800223X, 2008.

Bindschadler, R. A. and Scambos, T. A.: Satellite-Image-Derived Velocity Field of an Antarctic Ice Stream, Science, 252, 242–246, https://doi.org/10.1126/science.252.5003.242, https://science.sciencemag.org/content/252/5003/242, 1991.

Bottomley, J. T.: Flow of Viscous Materials—A Model Glacier, Nature, 21, 159–159, https://doi.org/10.1038/021159a0, http://www.nature.com/articles/021159a0, number: 529 Publisher: Nature Publishing Group, 1879.

Box, J. E., Colgan, W. T., Wouters, B., Burgess, D. O., O'Neel, S., Thomson, L. I., and Mernild, S. H.: Global sea-level contribution from Arctic land ice: 1971–2017, Environmental Research Letters, 13, 125 012, https://doi.org/10.1088/1748-9326/aaf2ed, https://doi.org/10.1088%2F1748-9326%2Faaf2ed, publisher: IOP Publishing, 2018.

Buchhave, P.: Particle image velocimetry—status and trends, Experimental Thermal and Fluid Science, 5, 586–604, https://doi.org/10.1016/0894-1777(92)90016-X, http://www.sciencedirect.com/science/article/pii/089417779290016X, 1992.

Bury, J. T., Mark, B. G., McKenzie, J. M., French, A., Baraer, M., Huh, K. I., Zapata Luyo, M. A., and Gómez López, R. J.: Glacier recession and human vulnerability in the Yanamarey watershed of the Cordillera Blanca, Peru, Climatic Change, 105, 179–206, https://doi.org/10.1007/s10584-010-9870-1, https://doi.org/10.1007/s10584-010-9870-1, 2011.

Chadwell, C. D.: Reliability analysis for design of stake networks to measure glacier surface velocity, Journal of Glaciology, 45, 154–164, https://doi.org/10.3189/S0022143000003130, http://www.cambridge.org/core/journals/journal-of-glaciology/article/reliability-analysis-for-design-of-stake-networks-to-measure-glacier-surface-velocity/F342FD59DA4D2EA6689383D677351269, publisher: Cambridge University Press, 1999.

Chevallier, P., Pouyaud, B., Suarez, W., and Condom, T.: Climate change threats to environment in the tropical Andes: glaciers and water resources, Regional Environmental Change, 11, 179–187, https://doi.org/10.1007/s10113-010-0177-6, http://link.springer.com/10.1007/s10113-010-0177-6, 2011.

Cuffey, K. M. and Paterson, W. S. B.: The Physics of Glaciers, Academic Press, google-Books-ID: Jca2v1u1EKEC, 2010.

Darji, S., Shah, R. D., Oza, S., and Bahuguna, I. M.: Inter-Comparison of Various Feature Tracking Tools Deriving Glacier Ice Velocity, 7, 8, 2018.

Davies, B. J. and Glasser, N. F.: Accelerating shrinkage of Patagonian glaciers from the Little Ice Age (~AD 1870) to 2011, Journal of Glaciology, 58, 1063–1084, https://doi.org/10.3189/2012JoG12J026, https://www.cambridge.org/core/journals/journal-of-glaciology/article/accelerating-shrinkage-of-patagonian-glaciers-from-the-little-ice-age-ad-1870-to-2011/933AF3AB94615A1E7AACF85510FF7FD1, 2012.

Deeley, R. M. and Parr, P. H.: XVI. The Hintereis Glacier, The London, Edinburgh, and Dublin Philosophical Magazine and Journal of Science, 27, 153–176, publisher: Taylor & Francis, 1914.

Drusch, M., Del Bello, U., Carlier, S., Colin, O., Fernandez, V., Gascon, F., Hoersch, B., Isola, C., Laberinti, P., Martimort, P., Meygret, A., Spoto, F., Sy, O., Marchese, F., and Bargellini, P.: Sentinel-2: ESA's Optical High-Resolution Mission for GMES Operational Services, Remote Sensing of Environment, 120, 25–36, https://doi.org/10.1016/j.rse.2011.11.026, http://www.sciencedirect.com/science/article/pii/S0034425712000636, 2012.

Earl, L. and Gardner, A.: A satellite-derived glacier inventory for North Asia, Annals of Glaciology, 57, 50–60, https://doi.org/10.3189/2016AoG71A008, http://www.cambridge.org/core/journals/annals-of-glaciology/article/satellitederived-glacier-inventory-for-north-asia/9CFCE79604C90AECCCAA5E0308D91B93, publisher: Cambridge University Press, 2016.

Fahnestock, M., Scambos, T., Moon, T., Gardner, A., Haran, T., and Klinger, M.: Rapid large-area mapping of ice flow using Landsat 8, Remote Sensing of Environment, 185, 84–94, https://doi.org/10.1016/j.rse.2015.11.023, http://www.sciencedirect.com/science/article/pii/S003442571530211X, 2016.

Farinotti, D., Huss, M., Fürst, J. J., Landmann, J., Machguth, H., Maussion, F., and Pandit, A.: A consensus estimate for the ice thickness distribution of all glaciers on Earth, Nature Geoscience, 12, 168, https://doi.org/10.1038/s41561-019-0300-3, https://www-nature-com.ezp3.lib.umn.edu/articles/s41561-019-0300-3, 2019.

Farr, T. G., Rosen, P. A., Caro, E., Crippen, R., Duren, R., Hensley, S., Kobrick, M., Paller, M., Rodriguez, E., Roth, L., Seal, D., Shaffer, S., Shimada, J., Umland, J., Werner, M., Oskin, M., Burbank, D., and Alsdorf, D.: The Shuttle Radar Topography Mission, Reviews of Geophysics, 45, https://doi.org/10.1029/2005RG000183, http://agupubs.onlinelibrary.wiley.com/doi/abs/10.1029/2005RG000183, _eprint: https://onlinelibrary.wiley.com/doi/pdf/10.1029/2005RG000183, 2007.

Fitch, A., Kadyrov, A., Christmas, W., and Kittler, J.: Orientation Correlation, in: Procedings of the British Machine Vision Conference 2002, pp. 11.1–11.10, British Machine Vision Association, Cardiff, https://doi.org/10.5244/C.16.11, http://www.bmva.org/bmvc/2002/papers/95/index.html, 2002.

Forbes, J. D.: The Glacier Theory, google-Books-ID: wPoTAAAAQAAJ, 1840.

Forbes, J. D.: XII. Illustrations of the viscous theory of glacier motion. - Part I. Containing experiments on the flow of plastic bodies, and observations on the phenomena of lava streams, Philosophical Transactions of the Royal Society of London, 136, 143–155, https://doi.org/10.1098/rstl.1846.0013, https://royalsocietypublishing.org/doi/abs/10.1098/rstl.1846.0013, publisher: Royal Society, 1846.

Fowler, A.: Weertman, Lliboutry and the development of sliding theory, Journal of Glaciology, 56, 965–972, https://doi.org/10.3189/002214311796406112, https://www.cambridge.org/core/product/identifier/S0022143000213191/type/journal_article, 2010.

Frigo, M. and Johnson, S.: FFTW: an adaptive software architecture for the FFT, in: Proceedings of the 1998 IEEE International Conference on Acoustics, Speech and Signal Processing, ICASSP '98 (Cat. No.98CH36181), vol. 3, pp. 1381–1384, IEEE, Seattle, WA, USA, https://doi.org/10.1109/ICASSP.1998.681704, http://ieeexplore.ieee.org/document/681704/, 1998.

Frigo, M. and Johnson, S.: The Design and Implementation of FFTW3, Proceedings of the IEEE, 93, 216–231, https://doi.org/10.1109/JPROC.2004.840301, conference Name: Proceedings of the IEEE, 2005.

Gantayat, P., Kulkarni, A. V., and Srinivasan, J.: Estimation of ice thickness using surface velocities and slope: case study at Gangotri Glacier, India, Journal of Glaciology, 60, 277–282, https://doi.org/10.3189/2014JoG13J078, https://www.cambridge.org/core/product/identifier/S0022143000205327/type/journal_article, 2014.

Gardner, A., Fahnestock, M., and Scambos, T.: ITS_LIVE Regional Glacier and Ice Sheet Surface Velocities., doi:10.5067/6II6VW8LLWJ7, 2020.

Gardner, A. S., Moholdt, G., Scambos, T., Fahnstock, M., Ligtenberg, S., Broeke, M. v. d., and Nilsson, J.: Increased West Antarctic and unchanged East Antarctic ice discharge over the last 7 years, The Cryosphere, 12, 521–547, https://doi.org/https://doi.org/10.5194/tc-12-521-2018, https://www.the-cryosphere.net/12/521/2018/, publisher: Copernicus GmbH, 2018.

Ginot, P., Schotterer, U., Stichler, W., Godoi, M. A., Francou, B., and Schwikowski, M.: Influence of the Tungurahua eruption on the ice core records of Chimborazo, Ecuador, The Cryosphere, 4, 561–568, https://doi.org/https://doi.org/10.5194/tc-4-561-2010, https://www.the-cryosphere.net/4/561/2010/, publisher: Copernicus GmbH, 2010.

Grant, I.: Particle image velocimetry: A review, Proceedings of the Institution of Mechanical Engineers, Part C: Journal of Mechanical Engineering Science, 211, 55–76, https://doi.org/10.1243/0954406971521665, https://doi.org/10.1243/0954406971521665, publisher: IMECHE, 1997.

Haeberli, W. and Hoelzle, M.: Application of inventory data for estimating characteristics of and regional climate-change effects on mountain glaciers: a pilot study with the European Alps, Annals of Glaciology, 21, 206–212, https://doi.org/10.3189/S0260305500015834, http://www.cambridge.org/core/journals/annals-of-glaciology/article/application-of-inventory-data-for-estimating-characteristics-of-and-regional-climatechange-effects-on-mountain-glaciers-a-pilot-study-with-the-eur 2F94393AD2866405FF3490C74D4EAE2D, publisher: Cambridge University Press, 1995.

Harris, A.: Thermal Remote Sensing of Active Volcanoes: A User's Manual, Cambridge University Press, google-Books-ID: xY4oYzbH0ooC, 2013.

Heid, T. and Kääb, A.: Evaluation of existing image matching methods for deriving glacier surface displacements globally from optical satellite imagery, Remote Sensing of Environment, 118, 339–355, https://doi.org/10.1016/j.rse.2011.11.024, http://www.sciencedirect.com/science/article/pii/S0034425711004214, 2012a.

Heid, T. and Kääb, A.: Repeat optical satellite images reveal widespread and long term decrease in land-terminating glacier speeds, The Cryosphere, 6, 467–478, https://doi.org/10.5194/tc-6-467-2012, https://www.the-cryosphere.net/6/467/2012/, 2012b.

Hooke, R. L., Calla, P., Holmlund, P., Nilsson, M., and Stroeven, A.: A 3 Year Record of Seasonal Variations in Surface Velocity, StorglaciÄren, Sweden, Journal of Glaciology, 35, 235–247, https://doi.org/10.3189/S0022143000004561, http://www.cambridge.org/core/journals/journal-of-glaciology/article/3-year-record-of-seasonal-variations-in-surface-velocity-storglaciaren-sweden/2BF67175ACC7E8843B2AC980C4804F4A, publisher: Cambridge University Press, 1989.

How, P., Hulton, N. R. J., Buie, L., and Benn, D. I.: PyTrx: A Python-Based Monoscopic Terrestrial Photogrammetry Toolset for Glaciology, Frontiers in Earth Science, 8, https://doi.org/10.3389/feart.2020.00021, https://www.frontiersin.org/articles/10.3389/feart.2020.00021/full, publisher: Frontiers, 2020.

Howat, I. M., Negrete, A., and Smith, B.: The Greenland Ice Mapping Project (GIMP) land classification and surface elevation data sets, https://doi.org/10.5194/tc-8-1509-2014, 2014.

Howat, I. M., Porter, C., Smith, B. E., Noh, M.-J., and Morin, P.: The Reference Elevation Model of Antarctica, The Cryosphere, 13, 665–674, https://doi.org/https://doi.org/10.5194/tc-13-665-2019, https://tc.copernicus.org/articles/13/665/2019/, publisher: Copernicus GmbH, 2019.

Hui, F., Cheng, X., Liu, Y., Zhang, Y., Ye, Y., Wang, X., Li, Z., Wang, K., Zhan, Z., Guo, J., Huang, H., Li, X., Guo, Z., and Gong, P.: An improved Landsat Image Mosaic of Antarctica, Science China Earth Sciences, 56, 1–12, https://doi.org/10.1007/s11430-012-4481-5, https://doi.org/10.1007/s11430-012-4481-5, 2013.

James, M. R., How, P., and Wynn, P. M.: Pointcatcher software: analysis of glacial time-lapse photography and integration with multitemporal digital elevation models, Journal of Glaciology, 62, 159–169, https://doi.org/10.1017/jog.2016.27, http://www.cambridge.org/core/journals/journal-of-glaciology/article/pointcatcher-software-analysis-of-glacial-timelapse-photography-and-integration-with-multitemporal-digital-elevation-models/23EC92804DE7C5EED7229D0ACE31D90B, publisher: Cambridge University Press, 2016.

Jawak, S. D., Kumar, S., Luis, A. J., Bartanwala, M., Tummala, S., and Pandey, A. C.: Evaluation of Geospatial Tools for Generating Accurate Glacier Velocity Maps from Optical Remote Sensing Data, Proceedings, 2, 341, https://doi.org/10.3390/ecrs-2-05154, https://www.mdpi.com/2504-3900/2/7/341, 2018.

Jiskoot, H.: Dynamics of Glaciers, in: Encyclopedia of Snow, Ice and Glaciers, edited by Singh, V. P., Singh, P., and Haritashya, U. K., pp. 245–256, Springer Netherlands, Dordrecht, https://doi.org/10.1007/978-90-481-2642-2_127, https://doi.org/10.1007/978-90-481-2642-2_127, 2011.

Kamb, B. and Echelmeyer, K. A.: Stress-gradient coupling in glacier flow: I. Longitudinal averaging of the influence of ice thickness and surface slope, Journal of Glaciology, 32, 267–284, publisher: Cambridge University Press, 1986.

Kamb, B. and LaChapelle, E.: Direct Observation of the Mechanism of Glacier Sliding Over Bedrock*, Journal of Glaciology, 5, 159–172, https://doi.org/10.3189/S0022143000028756, http://www.cambridge.org/core/journals/journal-of-glaciology/article/direct-observation-of-the-mechanism-of-glacier-sliding-over-bedrock/A032752BFEA9BB2628AC95966D72C332, publisher: Cambridge University Press, 1964.

Klemas, V. V.: The Role of Remote Sensing in Predicting and Determining Coastal Storm Impacts, Journal of Coastal Research, 25, 1264–1275, https://doi.org/10.2112/08-1146.1, https://meridian.allenpress.com/jcr/article/25/6(256)/1264/28316/The-Role-of-Remote-Sensing-in-Predicting-and, publisher: Allen Press, 2009.

Kobayashi, T. and Otsu, N.: Image Feature Extraction Using Gradient Local Auto-Correlations, Computer Vision - ECCV 2008, 10th European Conference on Computer Vision, 2008.

Kääb, A. and Vollmer, M.: Surface Geometry, Thickness Changes and Flow Fields on Creeping Mountain Permafrost: Automatic Extraction by Digital Image Analysis, Permafrost and Periglacial Processes, 11, 315–326, https://doi.org/10.1002/1099-1530(200012)11:4<315::AID-PPP365>3.0.CO;2-J, http://onlinelibrary.wiley.com/doi/abs/10.1002/1099-1530%28200012%2911%3A4%3C315%3A%3AAID-PPP365%3E3.0.CO%3B2-J, _eprint: https://onlinelibrary.wiley.com/doi/pdf/10.1002/1099-1530%28200012%2911%3A4%3C315%3A%3AAID-PPP365%3E3.0.CO%3B2-J, 2000.

Kääb, A., Winsvold, S. H., Altena, B., Nuth, C., Nagler, T., and Wuite, J.: Glacier Remote Sensing Using Sentinel-2. Part I: Radiometric and Geometric Performance, and Application to Ice Velocity, Remote Sensing, 8, 598, https://doi.org/10.3390/rs8070598, https://www.mdpi.com/2072-4292/8/7/598, number: 7 Publisher: Multidisciplinary Digital Publishing Institute, 2016.

La Frenierre, J. and Mark, B. G.: Detecting Patterns of Climate Change at Volcán Chimborazo, Ecuador, by Integrating Instrumental Data, Public Observations, and Glacier Change Analysis, Annals of the American Association of Geographers, 107, 979–997, https://doi.org/10.1080/24694452.2016.1270185, https://doi.org/10.1080/24694452.2016.1270185, publisher: Taylor & Francis _eprint: https://doi.org/10.1080/24694452.2016.1270185, 2017.

Lee, R. M., Yue, H., Rappel, W.-J., and Losert, W.: Data from: Inferring single cell behavior from large-scale epithelial sheet migration patterns, https://doi.org/https://doi.org/10.13016/M2855R, http://drum.lib.umd.edu/handle/1903/19190, accepted: 2017-04-12T17:46:08Z type: dataset, 2017.

Leprince, S., Ayoub, F., Klinger, Y., and Avouac, J.-P.: Co-Registration of Optically Sensed Images and Correlation (COSI-Corr): an operational methodology for ground deformation measurements, in: 2007 IEEE International Geoscience and Remote Sensing Symposium, pp. 1943–1946, IEEE, Barcelona, Spain, https://doi.org/10.1109/IGARSS.2007.4423207, http://ieeexplore.ieee.org/document/4423207/, 2007a.

Leprince, S., Barbot, S., Ayoub, F., and Avouac, J.-P.: Automatic and Precise Orthorectification, Coregistration, and Subpixel Correlation of Satellite Images, Application to Ground Deformation Measurements, IEEE Transactions on Geoscience and Remote Sensing, 45, 1529–1558, https://doi.org/10.1109/TGRS.2006.888937, 2007b.

Linsbauer, A., Paul, F., and Haeberli, W.: Modeling glacier thickness distribution and bed topography over entire mountain ranges with GlabTop: Application of a fast and robust approach, Journal of Geophysical Research: Earth Surface, 117, https://doi.org/10.1029/2011JF002313, http://agupubs.pericles.prod.literatumonline.com/doi/abs/10.1029/2011JF002313, _eprint: https://onlinelibrary.wiley.com/doi/pdf/10.1029/2011JF002313, 2012.

Mair, D., Willis, I., Fischer, U. H., Hubbard, B., Nienow, P., and Hubbard, A.: Hydrological controls on patterns of surface, internal and basal motion during three "spring events": Haut Glacier d'Arolla, Switzerland, Journal of Glaciology, 49, 555–567, https://doi.org/10.3189/172756503781830467, http://www.cambridge.org/core/journals/journal-of-glaciology/article/hydrological-controls-on-patterns-of-surface-internal-and-basal-motion-during-three-spring-events-haut-glacier-darolla-switzerland/9C10F4D8C42938F396AEF8E372F55247, publisher: Cambridge University Press, 2003.

Marc, O. and Hovius, N.: Amalgamation in landslide maps: effects and automatic detection, Natural Hazards and Earth System Sciences, 15, 723–733, https://doi.org/https://doi.org/10.5194/nhess-15-723-2015, https://www.nat-hazards-earth-syst-sci.net/15/723/2015/nhess-15-723-2015.html, publisher: Copernicus GmbH, 2015.

Meier, M. F. and Tangborn, W. V.: Net Budget and Flow of South Cascade Glacier, Washington, Journal of Glaciology, 5, 547–566, https://doi.org/10.3189/S0022143000018608, http://www.cambridge.org/core/journals/journal-of-glaciology/article/net-budget-and-flow-of-south-cascade-glacier-washington/440E67FA2A6041F58689DDBB65733502, publisher: Cambridge University Press, 1965.

Messerli, A. and Grinsted, A.: Image georectification and feature tracking toolbox: ImGRAFT, Geoscientific Instrumentation, Methods and Data Systems, 4, 23–34, https://doi.org/10.5194/gi-4-23-2015, https://www.geosci-instrum-method-data-syst.net/4/23/2015/, 2015.

Metternicht, G., Hurni, L., and Gogu, R.: Remote sensing of landslides: An analysis of the potential contribution to geo-spatial systems for hazard assessment in mountainous environments, Remote Sensing of Environment, 98, 284–303, https://doi.org/10.1016/j.rse.2005.08.004, http://www.sciencedirect.com/science/article/pii/S0034425705002506, 2005.

Millan, R.: Ice thickness and bed elevation of the Patagonian Icefields, https://doi.org/10.7280/d11q17, https://dash.lib.uci.edu/stash/dataset/doi:10.7280/D11Q17, type: dataset, 2019.

Millan, R., Mouginot, J., Rabatel, A., Jeong, S., Cusicanqui, D., Derkacheva, A., and Chekki, M.: Mapping Surface Flow Velocity of Glaciers at Regional Scale Using a Multiple Sensors Approach, Remote Sensing, 11, 2498, https://doi.org/10.3390/rs11212498, https://www.mdpi.com/2072-4292/11/21/2498, number: 21 Publisher: Multidisciplinary Digital Publishing Institute, 2019.

Minchew, B. M., Simons, M., Riel, B., and Milillo, P.: Tidally induced variations in vertical and horizontal motion on Rutford Ice Stream, West Antarctica, inferred from remotely sensed observations, Journal of Geophysical Research: Earth Surface, 122, 167–190, https://doi.org/10.1002/2016JF003971, http://agupubs.onlinelibrary.wiley.com/doi/abs/10.1002/2016JF003971, _eprint: https://onlinelibrary.wiley.com/doi/pdf/10.1002/2016JF003971, 2017.

Mote, T. L.: Greenland surface melt trends 1973–2007: Evidence of a large increase in 2007, Geophysical Research Letters, 34, https://doi.org/10.1029/2007GL031976, http://agupubs.onlinelibrary.wiley.com/doi/abs/10.1029/2007GL031976, _eprint: https://onlinelibrary.wiley.com/doi/pdf/10.1029/2007GL031976, 2007.

Mouginot, J. and Rignot, E.: Ice motion of the Patagonian Icefields of South America: 1984–2014, Geophysical Research Letters, 42, 1441–1449, https://doi.org/10.1002/2014GL062661, https://agupubs.onlinelibrary.wiley.com/doi/full/10.1002/2014GL062661, 2015.

Nagy, T. and Andreassen, L. M.: Glacier surface velocity mapping with Sentinel-2 imagery in Norway, 2019.

Nagy, T., Andreassen, L. M., Duller, R. A., and Gonzalez, P. J.: SenDiT: The Sentinel-2 Displacement Toolbox with Application to Glacier Surface Velocities, Remote Sensing, 11, 1151, https://doi.org/10.3390/rs11101151, https://www.mdpi.com/2072-4292/11/10/1151, number: 10 Publisher: Multidisciplinary Digital Publishing Institute, 2019.

Nye, J. F.: The Mechanics of Glacier Flow, Journal of Glaciology, 2, 82–93, https://doi.org/10.3189/S0022143000033967, http://www.cambridge.org/core/journals/journal-of-glaciology/article/mechanics-of-glacier-flow/5FB3C31120796459A837491ACB085F32, publisher: Cambridge University Press, 1952.

Nye, J. F.: Glacier sliding without cavitation in a linear viscous approximation, Proceedings of the Royal Society of London. A. Mathematical and Physical Sciences, 315, 381–403, publisher: The Royal Society London, 1970.

Oertel, M. and Süfke, F.: Two-dimensional dam-break wave analysis: particle image velocimetry versus optical flow, Journal of Hydraulic Research, 58, 326–334, https://doi.org/10.1080/00221686.2019.1579114, https://doi.org/10.1080/00221686.2019.1579114, publisher: Taylor & Francis _eprint: https://doi.org/10.1080/00221686.2019.1579114, 2020.

Pfeffer, W. T., Arendt, A. A., Bliss, A., Bolch, T., Cogley, J. G., Gardner, A. S., Hagen, J.-O., Hock, R., Kaser, G., Kienholz, C., Miles, E. S., Moholdt, G., Mölg, N., Paul, F., Radić, V., Rastner, P., Raup, B. H., Rich, J., Sharp, M. J., and Consortium, T. R.: The Randolph Glacier Inventory: a globally complete inventory of glaciers, Journal of Glaciology, 60, 537–552, https://doi.org/10.3189/2014JoG13J176, http://www.cambridge.org/core/journals/journal-of-glaciology/article/randolph-glacier-inventory-a-globally-complete-inventory-of-glaciers/730D4CC76E0E3EC1832FA3F4D90691CE, publisher: Cambridge University Press, 2014.

Porter, C., Morin, P., Howat, I., Noh, M.-J., Bates, B., Peterman, K., Keesey, S., Schlenk, M., Gardiner, J., Tomko, K., Willis, M., Kelleher, C., Cloutier, M., Husby, E., Foga, S., Nakamura, H., Platson, M., Wethington, M., Williamson, C., Bauer, G., Enos, J., Arnold, G., Kramer, W., Becker, P., Doshi, A., D'Souza, C., Cummens, P., Laurier, F., and Bojesen, M.: ArcticDEM, https://doi.org/10.7910/DVN/OHHUKH, https://dataverse.harvard.edu/dataset.xhtml?persistentId=doi:10.7910/DVN/OHHUKH, publisher: Harvard Dataverse type: dataset, 2018.

Rabatel, A., Dedieu, J.-P., Thibert, E., Letréguilly, A., and Vincent, C.: 25 years (1981–2005) of equilibrium-line altitude and mass-balance reconstruction on Glacier Blanc, French Alps, using remote-sensing methods and meteorological data, Journal of Glaciology, 54, 307–314, https://doi.org/10.3189/002214308784886063, http://www.cambridge.org/core/journals/journal-of-glaciology/article/25-years-19812005-of-equilibriumline-altitude-and-massbalance-reconstruction-on-glacier-blanc-french-alps-using-remotesensing-methods-and-me DB04ED9DE41C79FCA126917511C8A08E, publisher: Cambridge University Press, 2008.

Rabatel, A., Sanchez, O., Vincent, C., and Six, D.: Estimation of Glacier Thickness From Surface Mass Balance and Ice Flow Velocities: A Case Study on Argentière Glacier, France, Frontiers in Earth Science, 6, https://doi.org/10.3389/feart.2018.00112, https://www.frontiersin.org/articles/10.3389/feart.2018.00112/full, publisher: Frontiers, 2018.

Raffel, M., Willert, C. E., Scarano, F., Kähler, C. J., Wereley, S. T., and Kompenhans, J.: Particle Image Velocimetry: A Practical Guide, Springer, google-Books-ID: wk9UDwAAQBAJ, 2018.

Ramirez, E., Hoffmann, G., Taupin, J. D., Francou, B., Ribstein, P., Caillon, N., Ferron, F. A., Landais, A., Petit, J. R., Pouyaud, B., Schotterer, U., Simoes, J. C., and Stievenard, M.: A new Andean deep ice core from Nevado Illimani (6350 m), Bolivia, Earth and Planetary Science Letters, 212, 337–350, https://doi.org/10.1016/S0012-821X(03)00240-1, http://www.sciencedirect.com/science/article/pii/S0012821X03002401, 2003.

Rhee, J., Im, J., and Carbone, G. J.: Monitoring agricultural drought for arid and humid regions using multi-sensor remote sensing data, Remote Sensing of Environment, 114, 2875–2887, https://doi.org/10.1016/j.rse.2010.07.005, http://www.sciencedirect.com/science/article/pii/S003442571000221X, 2010.

Rignot, E., Mouginot, J., and Scheuchl, B.: Ice Flow of the Antarctic Ice Sheet, Science, 333, 1427–1430, https://doi.org/10.1126/science.1208336, https://science.sciencemag.org/content/333/6048/1427, publisher: American Association for the Advancement of Science Section: Report, 2011.

Saberi, L., McLaughlin, R. T., Ng, G.-H. C., Frenierre, J. L., Wickert, A. D., Baraer, M., Zhi, W., Li, L., and Mark, B. G.: Multi-scale temporal variability in meltwater contributions in a tropical glacierized watershed, Hydrology and Earth System Sciences, 23, 405–425, https://doi.org/https://doi.org/10.5194/hess-23-405-2019, https://www.hydrol-earth-syst-sci.net/23/405/2019/hess-23-405-2019.html, publisher: Copernicus GmbH, 2019.

Scambos, M. F. T.: Global Land Ice Velocity Extraction from Landsat 8 (GoLIVE), https://doi.org/10.7265/N5ZP442B, https://nsidc.org/data/nsidc-0710, type: dataset, 2016.

Scambos, T. A., Dutkiewicz, M. J., Wilson, J. C., and Bindschadler, R. A.: Application of image cross-correlation to the measurement of glacier velocity using satellite image data, Remote Sensing of Environment, 42, 177–186, https://doi.org/10.1016/0034-4257(92)90101-O, http://www.sciencedirect.com/science/article/pii/003442579290101O, 1992.

Scambos, T. A., Haran, T. M., Fahnestock, M. A., Painter, T. H., and Bohlander, J.: MODIS-based Mosaic of Antarctica (MOA) data sets: Continent-wide surface morphology and snow grain size, Remote Sensing of Environment, 111, 242–257, https://doi.org/10.1016/j.rse.2006.12.020, http://www.sciencedirect.com/science/article/pii/S0034425707002854, 2007.

Schotterer, U., Grosjean, M., Stichler, W., Ginot, P., Kull, C., Bonnaveira, H., Francou, B., Gäggeler, H. W., Gallaire, R., Hoffmann, G., Pouyaud, B., Ramirez, E., Schwikowski, M., and Taupin, J. D.: Glaciers and Climate in the Andes between the Equator and 30° S: What is Recorded under Extreme Environmental Conditions?, Climatic Change, 59, 157–175, https://doi.org/10.1023/A:1024423719288, https://doi.org/10.1023/A:1024423719288, 2003.

Schwalbe, E. and Maas, H.-G.: The determination of high-resolution spatio-temporal glacier motion fields from time-lapse sequences, Earth Surface Dynamics, 5, 861–879, https://doi.org/10.5194/esurf-5-861-2017, https://www.earth-surf-dynam.net/5/861/2017/, 2017.

Shean, D.: dshean/vmap: Zenodo DOI release, https://doi.org/10.5281/zenodo.3243479, https://zenodo.org/record/3243479#.XwiOvihKhPY, 2019.

Sneed, W. A. and Hamilton, G. S.: Evolution of melt pond volume on the surface of the Greenland Ice Sheet, Geophysical Research Letters, 34, https://doi.org/10.1029/2006GL028697, http://agupubs.onlinelibrary.wiley.com/doi/abs/10.1029/2006GL028697, _eprint: https://onlinelibrary.wiley.com/doi/pdf/10.1029/2006GL028697, 2007.

Stearns, L. A., Smith, B. E., and Hamilton, G. S.: Increased flow speed on a large East Antarctic outlet glacier caused by subglacial floods, Nature Geoscience, 1, 827–831, https://doi.org/10.1038/ngeo356, http://www.nature.com/articles/ngeo356, number: 12 Publisher: Nature Publishing Group, 2008.

Stocker, T. F., Qin, D., Plattner, G.-K., Tignor, M., Allen, S. K., Boschung, J., Nauels, A., Xia, Y., Bex, V., and Midgley, P. M.: Climate change 2013: The physical science basis, Contribution of working group I to the fifth assessment report of the intergovernmental panel on climate change, 1535, publisher: Cambridge university press Cambridge, United Kingdom and New York, NY, USA, 2013.

Sveen, J. K.: An introduction to MatPIV v. 1.6.1, https://www.duo.uio.no/handle/10852/10196, accepted: 2013-03-12T08:18:23Z Publisher: Matematisk Institutt, Universitetet i Oslo, 2004.

Sveen, J. K. and Cowen, E. A.: Quantitative imaging techniques and their application to wavy flows, in: PIV and Water Waves, vol. Volume 9 of *Advances in Coastal and Ocean Engineering*, pp. 1–49, WORLD SCIENTIFIC, https://doi.org/10.1142/9789812796615_0001, https://www.worldscientific.com/doi/abs/10.1142/9789812796615_0001, 2004.

Thielicke, W. and Stamhuis, E.: PIVlab – Towards User-friendly, Affordable and Accurate Digital Particle Image Velocimetry in MATLAB, Journal of Open Research Software, 2, e30, https://doi.org/10.5334/jors.bl, http://openresearchsoftware.metajnl.com/articles/10.5334/jors.bl/, number: 1 Publisher: Ubiquity Press, 2014.

Thompson, L. G., Mosley-Thompson, E., Davis, M. E., and Brecher, H. H.: Tropical glaciers, recorders and indicators of climate change, are disappearing globally, Annals of Glaciology, 52, 23–34, https://doi.org/10.3189/172756411799096231, https://www.cambridge.org/core/product/identifier/S0260305500250957/type/journal_article, 2011.

Tralli, D. M., Blom, R. G., Zlotnicki, V., Donnellan, A., and Evans, D. L.: Satellite remote sensing of earthquake, volcano, flood, landslide and coastal inundation hazards, ISPRS Journal of Photogrammetry and Remote Sensing, 59, 185–198, https://doi.org/10.1016/j.isprsjprs.2005.02.002, http://www.sciencedirect.com/science/article/pii/S0924271605000043, 2005.

Van Wyk de Vries, M.: Glacier Image Velocimetry (GIV), https://doi.org/10.5281/zenodo.4159875, https://zenodo.org/record/4144839#.X5l7OtD7RPY, 2020a.

Van Wyk de Vries, M.: Glacier Image Velocimetry (GIV) app, https://doi.org/10.5281/zenodo.4147589, https://zenodo.org/record/4144854#.X5l7Z9D7RPY, 2020b.

Van Wyk de Vries, M.: Ice velocity to thickness inversion, https://doi.org/10.5281/zenodo.3939211, https://zenodo.org/record/3939211#.XwigLyhKhPY, language: eng, 2020c.

Vergara, W., Deeb, A., Valencia, A., Bradley, R., Francou, B., Zarzar, A., Grünwaldt, A., and Haeussling, S.: Economic impacts of rapid glacier retreat in the Andes, Eos, Transactions American Geophysical Union, 88, 261–264, https://doi.org/10.1029/2007EO250001, http://agupubs.onlinelibrary.wiley.com/doi/abs/10.1029/2007EO250001, _eprint: https://onlinelibrary.wiley.com/doi/pdf/10.1029/2007EO250001, 2007.

Wal, R. S. W. v. d., Boot, W., Broeke, M. R. v. d., Smeets, C. J. P. P., Reijmer, C. H., Donker, J. J. A., and Oerlemans, J.: Large and Rapid Melt-Induced Velocity Changes in the Ablation Zone of the Greenland Ice Sheet, Science, 321, 111–113, https://doi.org/10.1126/science.1158540, https://science.sciencemag.org/content/321/5885/111, publisher: American Association for the Advancement of Science Section: Report, 2008.

Warren, C. R., Rivera, A., and Post, A.: Greatest Holocene advance of Glaciar Pio XI, Chilean Patagonia: possible causes, Annals of Glaciology, 24, 11–15, https://doi.org/10.3189/S026030550001185X, http://www.cambridge.org/core/journals/annals-of-glaciology/article/greatest-holocene-advance-of-glaciar-pio-xi-chilean-patagonia-possible-causes/7F3D1F2DB75C6783DE33153C1D415905, publisher: Cambridge University Press, 1997.

Weertman, J.: On the Sliding of Glaciers, Journal of Glaciology, 3, 33–38, https://doi.org/10.3189/S0022143000024709, http://www.cambridge.org/core/journals/journal-of-glaciology/article/on-the-sliding-of-glaciers/E16342853EE9ED61ED1CDE79FE3BF4C5, publisher: Cambridge University Press, 1957.

Wickert, A. D.: The ALog: Inexpensive, Open-Source, Automated Data Collection in the Field, The Bulletin of the Ecological Society of America, 95, 166–176, https://doi.org/10.1890/0012-9623-95.2.68, https://esajournals.onlinelibrary.wiley.com/doi/abs/10.1890/0012-9623-95.2.68, _eprint: https://esajournals.onlinelibrary.wiley.com/doi/pdf/10.1890/0012-9623-95.2.68, 2014.

Wickert, A. D., Sandell, C. T., Schulz, B., and Ng, G.-H. C.: Open-source Arduino-compatible data loggers designed for field research, Hydrology and Earth System Sciences, 23, 2065–2076, https://doi.org/https://doi.org/10.5194/hess-23-2065-2019, https://www.hydrol-earth-syst-sci.net/23/2065/2019/, publisher: Copernicus GmbH, 2019.

Willis, M. J., Zheng, W., Durkin, W. J., Pritchard, M. E., Ramage, J. M., Dowdeswell, J. A., Benham, T. J., Bassford, R. P., Stearns, L. A., Glazovsky, A. F., Macheret, Y. Y., and Porter, C. C.: Massive destabilization of an Arctic ice cap, Earth and Planetary Science Letters, 502, 146–155, https://doi.org/10.1016/j.epsl.2018.08.049, http://www.sciencedirect.com/science/article/pii/S0012821X18305156, 2018.

Wright, R., Flynn, L., Garbeil, H., Harris, A., and Pilger, E.: Automated volcanic eruption detection using MODIS, Remote Sensing of Environment, 82, 135–155, https://doi.org/10.1016/S0034-4257(02)00030-5, http://www.sciencedirect.com/science/article/pii/S0034425702000305, 2002.

Yuwei, W. U., Jianqiao, H. E., Zhongming, G. U. O., and Anan, C.: Limitations in identifying the equilibrium-line altitude from the optical remote-sensing derived snowline in the Tien Shan, China, Journal of Glaciology, 60, 1093–1100, https://doi.org/10.3189/2014JoG13J221, http://www.cambridge.org/core/journals/journal-of-glaciology/article/limitations-in-identifying-the-equilibriumline-altitude-from-the-optical-remotesensing-derived-snowline-in-the-tien-shan-china/6B84B734744312D483016C99C6373356, publisher: Cambridge University Press, 2014.

Zheng, W., Pritchard, M. E., Willis, M. J., Tepes, P., Gourmelen, N., Benham, T. J., and Dowdeswell, J. A.: Accelerating glacier mass loss on Franz Josef Land, Russian Arctic, Remote Sensing of Environment, 211, 357–375, https://doi.org/10.1016/j.rse.2018.04.004, http://www.sciencedirect.com/science/article/pii/S0034425718301494, 2018.

Zheng, W., Durkin, W. J., Melkonian, A. K., and Pritchard, M. E.: Cryosphere And Remote Sensing Toolkit (CARST) v1.0.1, https://doi.org/10.5281/zenodo.3475693, https://zenodo.org/record/3475693#.XvSuS2hKhPZ, 2019a.

Zheng, W., Pritchard, M. E., Willis, M. J., and Stearns, L. A.: The Possible Transition From Glacial Surge to Ice Stream on Vavilov Ice Cap, Geophysical Research Letters, 46, 13 892–13 902, https://doi.org/10.1029/2019GL084948, http://agupubs.onlinelibrary.wiley.com/doi/abs/10.1029/2019GL084948, _eprint: https://onlinelibrary.wiley.com/doi/pdf/10.1029/2019GL084948, 2019b.